

Hard Thresholding Pursuit Algorithms for Least Absolute Deviations Problem

Jiao Xu^{1,2}, Peng Li^{1*}, Bing Zheng¹

Abstract. Least absolute deviations (LAD) is a statistical optimality criterion widely utilized in scenarios where a minority of measurements are contaminated by outliers of arbitrary magnitudes. In this paper, we delve into the robustness of the variant of adaptive iterative hard thresholding to outliers, known as graded fast hard thresholding pursuit (GFHTP₁) algorithm. Unlike the majority of the state-of-the-art algorithms in this field, GFHTP₁ does not require prior information about the signal's sparsity. Moreover, its design is parameterless, which not only simplifies the implementation process but also removes the intricacies of parameter optimization. Numerical experiments reveal that the GFHTP₁ algorithm consistently outperforms competing algorithms in terms of both robustness and computational efficiency.

Keywords and Phrases. Least absolute deviations; Hard thresholding pursuit; Outliers; Graded.

MSC 2020. 65F10, 65J20, 15A29, 94A12

1 Introduction

1.1 Problem Setup

Outliers are ubiquitous [17, 24, 39], for example sensor calibration [23], face recognition [12], video surveillance [19], and their magnitudes can be arbitrarily large [11]. When outliers are present, the least squares (LS) method tends to severely bias signal estimation by amplifying the impact of outliers through squared residuals. In contrast, the least absolute deviations (LAD) criterion is more robust to outliers by minimizing absolute residuals, but efficient and parameter-free algorithms for sparse-constrained LAD remain scarce. In this paper, we investigate the problem of sparse signal recovery from linear measurements that contain a constant fraction of gross, arbitrary errors. Specifically, given a fixed measurement matrix $\mathbf{A} \in \mathbb{R}^{m \times n}$ (with $m \ll n$), our task is to identify an s -sparse \mathbf{x}_0 that satisfies:

$$\mathbf{b} = \mathbf{A}\mathbf{x}_0 + \boldsymbol{\eta}, \quad (1.1)$$

where $\mathbf{b} \in \mathbb{R}^m$ is the known measured response vector, and $\boldsymbol{\eta}$ is the unknown outliers with support T and cardinality $|T| = pm \ll m$. The nonzero values of $\boldsymbol{\eta}$ are significantly larger than the nonzero components of the signal \mathbf{x}_0 .

Our goal is to recover \mathbf{x}_0 from the observations (1.1), noting that the outliers (or the residual) $\boldsymbol{\eta} = \mathbf{b} - \mathbf{A}\mathbf{x}_0$ is sparse, i.e., $\|\mathbf{b} - \mathbf{A}\mathbf{x}_0\|_0 < m$. Here the notation $\|\mathbf{x}\|_0 = |\{j \in [[n]] : |x_j| \neq 0\}|$ denotes the ℓ_0 -norm (count of nonzero entries). This leads to the following sparsity-constrained

* Corresponding author.

¹ School of Mathematics and Statistics, Lanzhou University, Lanzhou, 730000, People's Republic of China

² School of Mathematics and Statistics, Hubei Normal University, Huangshi, 435002, People's Republic of China
E-mail addresses: xujiao21@lzu.edu.cn, xujiao@hbnu.edu.cn (J. Xu), lp@lzu.edu.cn (P. Li), bzheng@lzu.edu.cn (B. Zheng)

problem:

$$\min_{\mathbf{x} \in \mathbb{R}^n} \|\mathbf{b} - \mathbf{Ax}\|_0, \text{ s.t. } \|\mathbf{x}\|_0 \leq s \quad (1.2)$$

with s being an integer estimate of the sparsity level of \mathbf{x} . Since optimizing the ℓ_0 -norm is NP-hard, we relax the residual term to the ℓ_1 -norm to obtain the computationally feasible sparse-constrained LAD model:

$$\min_{\mathbf{x} \in \mathbb{R}^n} \|\mathbf{b} - \mathbf{Ax}\|_1, \text{ s.t. } \|\mathbf{x}\|_0 \leq s. \quad (1.3)$$

Our primary objective is to develop an efficient, fast algorithm for solving this nonsmooth optimization problem by leveraging the hard thresholding pursuit (HTP) technique.

1.2 Related Work

Existing methods for sparse signal recovery under outliers can be categorized based on their ability to address three core challenges: outliers robustness, unknown sparsity, and computational efficiency. Below, we review relevant work and highlight their limitations relative to our research goals.

1.2.1 Least Absolute Deviations

We first recall the related work about LAD. It is well known that the traditional LS method $\min_{\mathbf{x} \in \mathbb{R}^n} \|\mathbf{b} - \mathbf{Ax}\|_2$ is recognized for its optimality in scenarios where the measurement noise follows a Gaussian distribution. However, in practical applications, noise often exhibits non-Gaussian characteristics. The LS method's effectiveness is contingent upon assumptions regarding the noise's structure or standard deviation [2], rendering it less reliable in the presence of impulsive noise, outliers, and other anomalies. In such cases, the LAD [1] emerges as a valuable alternative. LAD is a statistical optimality criterion and a robust optimization technique that seeks to approximate data by minimizing the sum of the absolute values of the residuals [3]. Dielman [13] has shown that LAD outperforms the LS method in scenarios involving impulsive noise, sparse noise, and outliers, primarily due to its robust nature. Unlike the LS method, which overweights large residuals, LAD treats all observations equally, making it suitable for data with arbitrary outliers.

LAD has been applied in the development of robust methods across various domains, including statistical communities [13], compressive sensing signal reconstruction [27], sparse representation-based face recognition [29], channel estimation [18], and image denoising [26]. However, LAD solvers that are sparsely constrained still face critical limitations. Li et al. [21] introduced an adaptive iterative hard thresholding (AIHT) algorithm, which performs subgradient descent followed by a hard thresholding operator $\mathcal{H}_s(\mathbf{x})$. This operator retains the largest s elements of \mathbf{x} in magnitude and sets the remainder to zero. Their algorithm is globally convergent under bounded noise but fails in the presence of outliers. Additionally, it requires prior knowledge of the sparsity s —a major drawback in practical applications. Recently, Xu et al. [31] proposed an algorithm to solve the aforementioned model (1.3) when both outliers and bounded noise exist, the algorithm is termed the projected subgradient decent (PSGD) algorithm. Nevertheless, the selection of the step size in this algorithm may not be optimal, as it relies on the actual signal—an issue that can lead to inaccuracies in its application.

Several scholars have also proposed convex or nonconvex relaxation methods for solving the LAD problem. For instance, Yang and Zhang [33] introduced an alternating direction algorithm to tackle the penalized (or regularized) LAD (PLAD or RLAD) model, which incorporates both the ℓ_1 regularized function $\|\mathbf{x}\|_1$ and the ℓ_1 loss function $\|\mathbf{b} - \mathbf{Ax}\|_1$ into the objective function. In 2013, Wang [30] conducted a theoretical analysis of this model, which is capable of handling cases where the error distribution is unknown or exhibits heavy tails, even for Cauchy distributions. The corresponding estimator demonstrates near-optimal performance with high probability. We also notice that Li et al. [20] have proposed a nonconvex minimization method with LAD constraint, which aims to solve an $\ell_1 - \alpha\ell_2$ minimization problem. They also contributed to the theoretical

analysis of the $\ell_1 - \alpha\ell_2$ minimization model. However, the theoretical analysis provided for the proposed model is not applicable to cases with outliers. Recently, Xu et al. [32] have presented a theoretical analysis for the unconstrained version of the $\ell_1 - \alpha\ell_2$ minimization model, which is valid when observations are corrupted by the outliers. Nevertheless, numerical experiments reveal that the model's performance degrades significantly when the outlier rate is high. Therefore, the objective of this paper is to develop an efficient method that remains robust to outliers, even when they are present in large proportions.

1.2.2 Hard Thresholding Algorithms

Another related work involves hard thresholding algorithms, which solve a sparsity-constrained LS model defined as:

$$\min_{\mathbf{x} \in \mathbb{R}^n} \|\mathbf{b} - \mathbf{Ax}\|_2^2, \text{ s.t. } \|\mathbf{x}\|_0 \leq s.$$

Here, the measured response vector $\mathbf{b} \in \mathbb{R}^m$ is given by

$$\mathbf{b} = \mathbf{Ax}_0 + \mathbf{e},$$

where $\mathbf{e} \in \mathbb{R}^m$ denotes the vector of bounded measurement errors (or bounded noise). Blumensath and Davies [4, 5] were the first to introduce the IHT algorithm for addressing sparse signal reconstruction problems with sparsity constraints. The IHT algorithm primarily employs the gradient descent and hard thresholding technique, demonstrating perfect performance in Gaussian noise scenarios. Subsequently, Blumensath and Davies [6] introduced the normalized IHT algorithm in 2010, which features an adaptive step size that optimally reduces the error at each iteration, thereby eliminating the reliance on the scaling of \mathbf{A} and ensuring convergence and stability. Recently, Gilbert et al. [15] introduced the nonlinear IHT algorithm and successfully applied it to the field of inverse scattering.

In 2011, Foucart [14] proposed the hard thresholding pursuit (HTP) algorithm by merging the IHT and compressive sensing matching pursuit [25] algorithms. The HTP algorithm iterates through two steps: (1) In the first step (candidate support selection), the support S^{k+1} is estimated using the support set of the output from the IHT process; (2) In the second step (pursuit), the expression of \mathbf{x}^{k+1} is obtained by solving an LS problem, with the solution restricted to the known support set S^{k+1} . Foucart [14] also presented a variant of the HTP algorithm—fast HTP (FHTP) algorithm, which employs gradient descent and restricts it to the known support set S^{k+1} in the second (pursuit) step. In 2016, Bouchot et al. [7] introduced the graded HTP (GHTP) algorithm, a natural complement to orthogonal matching pursuit [36] that operates without requiring prior estimation of the sparsity level. In the $(k+1)$ -th iteration, they determine the candidate support by taking the indices of the $k+1$ largest absolute entries of $\mathbf{x}^k + \mathbf{A}^\top(\mathbf{b} - \mathbf{Ax}^k)$. This method removed the requirement for prior knowledge of sparsity, but added an impractical stopping criterion: $\text{supp}(\mathbf{x}_0) \subset S^{k+1}$ (or $\|\mathbf{x}^{k+1} - \mathbf{x}_0\|_2 / \|\mathbf{x}_0\|_2 < \epsilon$).

Subsequently, some scholars also proposed some variants of the HTP algorithm. For instance, Yuan et al. [34] expanded upon HTP by proposing GraHTP, which generalizes the algorithm from compressed sensing to the broader framework of sparsity-constrained loss minimization for nonlinear problems. Additionally, Zhang et al. [37] also developed a conjugate gradient HTP algorithm, which integrates elements of HTP with the conjugate gradient IHT for sparse signal recovery. Zhou et al. [38] have also contributed to the field by introducing a Newton HTP algorithm that exhibits quadratic convergence properties. In recent advancements, Sun et al. [28] have leveraged the heavy ball method to enhance the efficiency of hard thresholding algorithms without escalating computational demands. This approach, known as the heavy-ball-based hard thresholding algorithm and the heavy-ball-based HTP algorithm. These studies collectively demonstrate the significant application of HTP in sparse signal recovery. As far as we know, there remains a gap in the literature regarding the adaptation of HTP algorithm to solve sparse-constrained least absolute deviations (LAD) problem with outliers.

1.3 Motivation and Contributions

We observe that the theoretical analysis presented in [21] encounters a limitation when dealing with observations containing outliers, as indicated by (1.1). Notably, RLAD-type models, such as those proposed in [30] and [32], may not perform optimally in the presence of high outlier rates. As a result, there is a need for the development of a more robust algorithm to overcome this limitation. The step size strategy employed in [31] for PSGD, which is contingent on the actual signal, may not be easily adaptable to practical situations. Additionally, the absence of a proposed stopping criterion by Xu et al. in [31] is somewhat regrettable. It would be beneficial to explore a step size that is more adaptable to real-world scenarios and to devise a stopping criterion that is both reasonable and practical. Consequently, we are interested in the following questions: (i) Can we establish the HTP algorithm to solve the sparsity-constrained LAD problem (1.3) when the sparsity of the original signal is unknown? (ii) Can we establish a global convergence analysis? (iii) Can we propose a reasonable stopping criterion?

Motivated by the aforementioned discussion, we propose the **graded fast hard thresholding pursuit (GFHTP₁)** algorithm for the sparsity-constrained LAD (1.3) with the observations (1.1). This paper's contributions are as follows:

- (a) **Parameter-Free Algorithm with Unknown Sparsity:** GFHTP₁ integrates FHTP's inner-iteration acceleration with GHTP's graded support growth (support size = k at outer iteration k), eliminating the need for prior knowledge of s . It uses a **truncated adaptive step size** (dependent only on small residual components, not the true signal) to suppress outliers, filling the gap of HTP-based methods for LAD.
- (b) **Rigorous Convergence Analysis:** We analyze convergence for two signal types:
 - For general s -sparse signals, we establish a linear error bound under the restricted isometry property (RIP₁).
 - For 'flat' signals satisfying $x_1^* \leq \lambda x_s^*$ ($\lambda \geq 1$, x_j^* is the non-increasing rearrangement of $|\mathbf{x}_0|$), we prove **exact recovery at the s -th outer iteration** ($\mathbf{x}^s = \mathbf{x}_0$) with high probability.
- (c) **Practical Stopping Criterion and Superior Performance:** We design a stopping criterion based on truncated residual ℓ_1 -norm ($\|(\mathbf{b} - \mathbf{Ax}^k) \odot (\mathbb{I}_{\{|b_i - (\mathbf{Ax}^k)_i| \leq \theta_\tau(|\mathbf{b} - \mathbf{Ax}^k|)\}})\|_1 \leq \epsilon_{\text{outer}}$), avoiding dependence on the true signal. Numerical experiments show GFHTP₁ outperforms PSGD and AIHT in success rates.

Our proposed algorithm builds upon the principles of FHTP [14], GHTP [37] and AIHT [21]. It effectively handles outliers by incorporating a truncated adaptive step size that exclusively relies on those small components of $\mathbf{b} - \mathbf{Au}^{k,l}$. Following this idea, we also design a highly efficient stopping criterion that promotes fast and precise convergence.

1.4 Organization and Notations

The remainder of this paper is structured as follows. Section 2 delves into the theoretical analysis of the GFHTP₁ algorithm. Section 3 gives the roadmap and keystone of our proofs. Section 4 examines the numerical performance of the proposed algorithms through experiments. Section 5 concludes the paper with a summary of the findings. Appendix A presents the proof of the general sparse signal recovery case. Appendix B provides the theoretical proof for the general sparse signal recovery case.

Throughout this paper, we use the following notations. Matrices are denoted by boldface capital letters, such as \mathbf{A} , while vectors are represented by boldface lowercase letters, for example, \mathbf{a} . Scalars are indicated by regular lowercase letters, such as a . The sign function $\text{sign}(\cdot)$ is defined as $\text{sign}(a) = a/|a|$ for $a \neq 0$, with $\text{sign}(0) = 0$. For any positive integer n , let $[[n]]$ represent the set

$\{1, \dots, n\}$. The notation $\mathbf{x}_\Omega \in \mathbb{R}^n$ refers to a vector where its elements are equal to \mathbf{x} for indices within the set Ω , and zero otherwise. Let Ω^c denote the complement of the index set Ω , which is defined as $\Omega^c = [[n]] \setminus \Omega$. Let \mathbf{A}_W denote the submatrix of \mathbf{A} obtained by keeping the rows of \mathbf{A} with indices in the set W . The indicator function $\mathbb{I}_B = 1$ if the event B holds, and $\mathbb{I}_B = 0$ otherwise. The notation \odot refers to the Hadamard product, and Φ is the cumulative distribution function of the standard Gaussian distribution. We use θ_τ to denote the τ -th quantile. We use $\mathbf{x}^* \in \mathbb{R}_+^n$ to represent the non-increasing rearrangement of the original signal $\mathbf{x}_0 \in \mathbb{R}^n$, meaning $x_1^* \geq x_2^* \geq \dots \geq x_n^* \geq 0$. There exists a permutation ν of $[[n]]$ such that $x_j^* = |x_{\nu(j)}|$ for all $j \in [[n]]$. For two index sets Ω and Ω' , $\Omega \Delta \Omega'$ denotes the symmetric difference of these sets, which is the union of their respective differences, i.e., $\Omega \Delta \Omega' = (\Omega \setminus \Omega') \cup (\Omega' \setminus \Omega)$.

2 Algorithms and Theoretical Results

In this section, we present the proposed algorithms in detail and rigorously analyze their convergence properties, providing clear theoretical support for their effectiveness in sparse signal recovery with outliers.

2.1 Our Algorithms

In this subsection, we design two efficient solving algorithms for the model 1.3. The first one needs the sparsity prior, while the second one addresses the limitation of requiring prior sparsity information.

2.1.1 Parameter Description

Before introducing the algorithms, we clarify the key parameters to ensure reproducibility and interpretability:

- (i) τ (quantile parameter): The quantile used to truncate outliers, satisfying $p < \tau < 1 - p$ (p is the outliers rate). Its role is to filter out large residual components (outliers) when calculating the step size, avoiding interference with iterative updates.
- (ii) $\theta_\tau(|\mathbf{b} - \mathbf{Ax}^k|)$: The τ -quantile of the absolute residual vector $|\mathbf{b} - \mathbf{Ax}^k|$, calculated based on the empirical distribution of the residual.
- (iii) $\mu_{k,l}$ (adaptive step size coefficient): A positive constant determining the step size scale, recommended to be initialized to 6 (verified by numerical experiments in Section 4.2) and adjusted within the range derived from theoretical conditions (see Theorem 2.2 and Remark 2.4).
- (iv) MaxIt: Maximum number of outer iterations, recommended to be set to $\text{ceil}(m/2)$ (m is the measurement dimension) to ensure the support set covers the true sparsity.
- (v) $\epsilon_{\text{outer}}, \epsilon_{\text{inner}}$: Termination thresholds for outer/inner iterations, controlling the convergence accuracy.

2.1.2 Fast Hard Thresholding Pursuit (FHTP₁) Algorithm

In this subsection, we design a fast algorithm for solving the nonsmooth sparsity-constrained LAD (1.3). To solve this optimization problem, we adopt the following alternating minimization scheme:

$$\begin{cases} S^{k+1} = \arg \min_{|S| \leq s} \|\mathbf{Ax}_S - \mathbf{b}\|_1, & \text{(Find the Candidate Support)} \\ \mathbf{x}^{k+1} = \arg \min_{\mathbf{x}: \text{supp}(\mathbf{x}) \subset S^{k+1}} \|\mathbf{Ax} - \mathbf{b}\|_1, & \text{(Update the Sparse Signal)} \end{cases} \quad (2.1)$$

The subproblems in the alternating minimization scheme (2.1) are solved either exactly or approximately, as detailed below:

(i) Finding the Candidate Support: We update the candidate support via the subgradient descent followed by a hard thresholding operator

$$\mathbf{u}^{k+1,1} := \mathcal{H}_s(\mathbf{x}^k + t_{k+1,0} \mathbf{A}^\top \text{sign}(\mathbf{b} - \mathbf{A}\mathbf{x}^k)), \quad S^{k+1} = \text{supp}(\mathbf{u}^{k+1,1}), \quad (2.2)$$

where $t_{k+1,0} > 0$ is a step size, and $-\mathbf{A}^\top \text{sign}(\mathbf{b} - \mathbf{A}\mathbf{x}^k)$ is the subgradient of the objective function $\|\mathbf{b} - \mathbf{A}\mathbf{x}^k\|_1$ at the current point \mathbf{x}^k .

(ii) Updating the Sparse Signal: The subproblem has no closed-form solution, so we solve it via subgradient descent with restriction to the given support

$$\mathbf{u}^{k+1,l+1} := (\mathbf{u}^{k+1,l} + t_{k+1,l} \mathbf{A}^\top \text{sign}(\mathbf{b} - \mathbf{A}\mathbf{u}^{k+1,l}))_{S^{k+1}}, \quad \mathbf{x}^{k+1} = \mathbf{u}^{k+1,L+1}. \quad (2.3)$$

In summary, our solving algorithm contains the following two iterative steps:

$$\begin{cases} \mathbf{u}^{k+1,1} := \mathcal{H}_s(\mathbf{x}^k + t_{k+1,0} \mathbf{A}^\top \text{sign}(\mathbf{b} - \mathbf{A}\mathbf{x}^k)), & S^{k+1} = \text{supp}(\mathbf{u}^{k+1,1}), \\ \mathbf{u}^{k+1,l+1} := (\mathbf{u}^{k+1,l} + t_{k+1,l} \mathbf{A}^\top \text{sign}(\mathbf{b} - \mathbf{A}\mathbf{u}^{k+1,l}))_{S^{k+1}}, & \mathbf{x}^{k+1} = \mathbf{u}^{k+1,L+1}. \end{cases} \quad (2.4)$$

Note that the idea of the first step is similar to that of HTP, which involves a gradient descent step followed by the hard thresholding operator \mathcal{H}_s . While the second step is similar to that of FHTP, which solves an LS with a constraint on the given support set. We can consider FHTP as being adapted to suit the nonsmooth model (1.3). Therefore we call this algorithm the Fast Hard Thresholding Pursuit for the ℓ_1 loss function (FHTP₁). The algorithm is presented in Algorithm 1.

Algorithm 1 Fast hard thresholding pursuit (FHTP₁) for solving (1.1)

Require: $\mathbf{A}, \mathbf{b}, \mathbf{x}^0, S^0 = \text{supp}(\mathbf{x}^0), s, \text{MaxIt}, L, \epsilon_{\text{outer}}, \epsilon_{\text{inner}}$

Ensure: \mathbf{x}

- 1: **Outer loop:**
- 2: **while** $0 \leq k \leq \text{MaxIt}$ and $S^k \neq S^{k-1}$ and $\|(\mathbf{b} - \mathbf{A}\mathbf{x}^k) \odot (\mathbb{I}_{\{|b_i - (\mathbf{A}\mathbf{x}^k)_i| \leq \theta_\tau(|\mathbf{b} - \mathbf{A}\mathbf{x}^k|)\}})_{i=1}^m\|_1 > \epsilon_{\text{outer}}$ **do**
- 3: Compute $t_{k+1,0} = \mu_{k+1,0} \sqrt{\frac{\pi}{2}} \|(\mathbf{b} - \mathbf{A}\mathbf{x}^k) \odot (\mathbb{I}_{\{|b_i - (\mathbf{A}\mathbf{x}^k)_i| \leq \theta_\tau(|\mathbf{b} - \mathbf{A}\mathbf{x}^k|)\}})_{i=1}^m\|_1$.
- 4: Compute $\mathbf{u}^{k+1,1} := \mathcal{H}_s(\mathbf{x}^k + t_{k+1,0} \mathbf{A}^\top \text{sign}(\mathbf{b} - \mathbf{A}\mathbf{x}^k))$ and $S^{k+1} = \text{supp}(\mathbf{u}^{k+1,1})$. Set $\mathbf{u}^{k+1,0} = \mathbf{x}^k$.
- 5: **Inner loop:**
- 6: **while** $1 \leq l \leq L$ and $\|\mathbf{u}^{k+1,l} - \mathbf{u}^{k+1,l-1}\|_2 / \|\mathbf{u}^{k+1,l-1}\|_2 > \epsilon_{\text{inner}}$ **do**
- 7: Compute $t_{k+1,l} = \mu_{k+1,l} \sqrt{\frac{\pi}{2}} \|(\mathbf{b} - \mathbf{A}\mathbf{u}^{k+1,l}) \odot (\mathbb{I}_{\{|b_i - (\mathbf{A}\mathbf{u}^{k+1,l})_i| \leq \theta_\tau(|\mathbf{b} - \mathbf{A}\mathbf{u}^{k+1,l}|)\}})_{i=1}^m\|_1$.
- 8: Compute $\mathbf{u}^{k+1,l+1} := (\mathbf{u}^{k+1,l} + t_{k+1,l} \mathbf{A}^\top \text{sign}(\mathbf{b} - \mathbf{A}\mathbf{u}^{k+1,l}))_{S^{k+1}}$.
- 9: Set $l := l + 1$.
- 10: **end while** and output $\mathbf{x}^{k+1} := \mathbf{u}^{k+1,L+1}$.
- 11: Set $k := k + 1$.
- 12: **end while**

Next, we design a stopping criterion. We set $\text{MaxIt} = \text{ceil}(m/2)$ and incorporate an appropriate stopping criterion, which is defined as follows:

- (i) For the inner iteration: $\|\mathbf{u}^{k+1,l+1} - \mathbf{u}^{k+1,l}\|_2 / \|\mathbf{u}^{k+1,l}\|_2 \leq \epsilon_{\text{inner}} = 10^{-8}$;
- (ii) For the outer iteration: $S^{k+1} = S^k$ or $\|(\mathbf{b} - \mathbf{A}\mathbf{x}^{k+1}) \odot (\mathbb{I}_{\{|b_i - (\mathbf{A}\mathbf{x}^{k+1})_i| \leq \theta_\tau(|\mathbf{b} - \mathbf{A}\mathbf{x}^{k+1}|)\}})_{i=1}^m\|_1 \leq \epsilon_{\text{outer}} = 10^{-4}$.

To conclude this subsection, we analyze the time complexity of Algorithm 1. It is mainly dominated by computing the hard thresholding operator $\mathcal{H}_s(\cdot)$ and $t_{k+1,l}$, and updating $\mathbf{u}^{k+1,l+1}$. We obtain that the time complexity for computing $\mathcal{H}_s(\cdot)$ is $\mathcal{O}(n \log s)$. Based on matrix multiplication and τ -quantile, the time complexity of calculating $t_{k+1,l}$ and $\mathbf{u}^{k+1,l+1}$ is $\mathcal{O}(sm + m \log m)$ and $\mathcal{O}(mn)$, respectively. Therefore the time complexity is $\mathcal{O}(k_{\text{outer}}(L(mn + m \log m) + n \log s))$, where k_{outer} denotes the number of outer iterations in Algorithm 1.

2.1.3 Graded Fast Hard Thresholding Pursuit (GFHTP₁) Algorithm

The FHTP₁ algorithm relies on prior knowledge of sparsity s , which limits its practical application. To address this, we propose the GFHTP₁ algorithm, which constructs a sequence of $(k+1)$ -sparse vectors (\mathbf{x}^{k+1}) with an index set that grows with each iteration:

$$\begin{cases} \mathbf{u}^{k+1,1} := \mathcal{H}_{k+1}(\mathbf{x}^k + t_{k+1,0} \mathbf{A}^\top \text{sign}(\mathbf{b} - \mathbf{A}\mathbf{x}^k)), & S^{k+1} = \text{supp}(\mathbf{u}^{k+1,1}), \\ \mathbf{u}^{k+1,l+1} := (\mathbf{u}^{k+1,l} + t_{k+1,l} \mathbf{A}^\top \text{sign}(\mathbf{b} - \mathbf{A}\mathbf{u}^{k+1,l}))_{S^{k+1}}, & \mathbf{x}^{k+1} = \mathbf{u}^{k+1,L+1}. \end{cases} \quad (2.5)$$

The algorithm is described in Algorithm 2.

Algorithm 2 Graded fast hard thresholding pursuit (GFHTP₁) for solving (1.1)

Require: $\mathbf{A}, \mathbf{b}, \mathbf{x}^0, S^0 = \text{supp}(\mathbf{x}^0), \text{MaxIt}, L, \epsilon_{\text{outer}}, \epsilon_{\text{inner}}$

Ensure: \mathbf{x}

```

1: Outer loop:
2: while  $k \leq \text{MaxIt}$  and  $\|(\mathbf{b} - \mathbf{A}\mathbf{x}^k) \odot (\mathbb{I}_{\{|b_i - (\mathbf{A}\mathbf{x}^k)_i| \leq \theta_\tau(|\mathbf{b} - \mathbf{A}\mathbf{x}^k|)\}})_{i=1}^m\|_1 > \epsilon_{\text{outer}}$  do
3:   Compute  $t_{k+1,0} = \mu_{k+1,0} \sqrt{\frac{\pi}{2}} \|(\mathbf{b} - \mathbf{A}\mathbf{x}^k) \odot (\mathbb{I}_{\{|b_i - (\mathbf{A}\mathbf{x}^k)_i| \leq \theta_\tau(|\mathbf{b} - \mathbf{A}\mathbf{x}^k|)\}})_{i=1}^m\|_1$ .
4:   Compute  $\mathbf{u}^{k+1,1} := \mathcal{H}_{k+1}(\mathbf{x}^k + t_{k+1,0} \mathbf{A}^\top \text{sign}(\mathbf{b} - \mathbf{A}\mathbf{x}^k))$  and  $S^{k+1} = \text{supp}(\mathbf{u}^{k+1,1})$ . Set  $\mathbf{u}^{k+1,0} = \mathbf{x}^k$ .
5: Inner loop:
6: while  $1 \leq l \leq L$  and  $\|\mathbf{u}^{k+1,l} - \mathbf{u}^{k+1,l-1}\|_2 / \|\mathbf{u}^{k+1,l-1}\|_2 > \epsilon_{\text{inner}}$  do
7:   Compute  $t_{k+1,l} = \mu_{k+1,l} \sqrt{\frac{\pi}{2}} \|(\mathbf{b} - \mathbf{A}\mathbf{u}^{k+1,l}) \odot (\mathbb{I}_{\{|b_i - (\mathbf{A}\mathbf{u}^{k+1,l})_i| \leq \theta_\tau(|\mathbf{b} - \mathbf{A}\mathbf{u}^{k+1,l}|)\}})_{i=1}^m\|_1$ .
8:   Compute  $\mathbf{u}^{k+1,l+1} := (\mathbf{u}^{k+1,l} + t_{k+1,l} \mathbf{A}^\top \text{sign}(\mathbf{b} - \mathbf{A}\mathbf{u}^{k+1,l}))_{S^{k+1}}$ .
9:   Set  $l := l + 1$ .
10: end while and output  $\mathbf{x}^{k+1} := \mathbf{u}^{k+1,L+1}$ .
11: Set  $k := k + 1$ .
12: end while

```

For the GFHTP₁ algorithm, we adopt its stopping criterion by removing the condition $S^{k+1} = S^k$ from the stopping criterion of the FHTP₁ algorithm.

2.2 Theoretical Results

We first derive error bounds for general sparse signals, then prove exact recovery for signals with specific constraints, and finally compare with state-of-the-art algorithms.

2.2.1 Foundational Assumption: Restricted 1-Isometry Property (RIP₁)

Definition 2.1. ([10, Inequation (1.8)]) A matrix $\mathbf{A} \in \mathbb{R}^{m \times n}$ is said to satisfy the RIP₁ of order s if there exists a small constant $\delta_s \in (0, 1)$ such that the inequality

$$(1 - \delta_s) \|\mathbf{x}\|_2 \leq \sqrt{\frac{\pi}{2}} \|\mathbf{A}\mathbf{x}\|_1 \leq (1 + \delta_s) \|\mathbf{x}\|_2 \quad (2.6)$$

holds for all vectors $\mathbf{x} \in \mathbb{R}^n$ with sparsity not exceeding s . The smallest constant δ_s that satisfies this inequality is known as the restricted 1-isometry constant (RIC₁).

What we should point out is that Gaussian random matrices satisfy RIP_1 with high probability (Lemma A.1), which is foundational for subsequent theorems.

2.2.2 Error Estimation for General Sparse Signals

Theorem 2.2. *Given an s -sparse vector $\mathbf{x}_0 \in \mathbb{R}^n$ and the measurements $\mathbf{b} = \mathbf{A}\mathbf{x}_0 + \boldsymbol{\eta}$, where $\boldsymbol{\eta}$ is a vector of outliers with support T and cardinality $|T| = pm$. Assume that the matrix \mathbf{A} satisfies RIP_1 with RIC_1 satisfying $0 < \delta_{2k+s-1} < 0.25$ and the fraction of outliers p satisfies $p < \frac{1}{2} - \frac{\delta_{2k+s-1}}{1-\delta_{2k+s-1}}$. Let $\{\mathbf{x}^k\}_{k=1}^\infty$ be the sequence produced by the GFHTP₁ algorithm, with adaptive step size*

$$t_{k,l} = \mu_{k,l} \sqrt{\frac{\pi}{2}} \|(\mathbf{b} - \mathbf{A}\mathbf{u}^{k,l}) \odot (\mathbb{I}_{\{|b_i - (\mathbf{A}\mathbf{u}^{k,l})_i| \leq \theta_\tau(|\mathbf{b} - \mathbf{A}\mathbf{u}^{k,l}|)\}})_{i=1}^m\|_1,$$

where $\mu_{k,l}$ satisfies the following inequality

$$\begin{aligned} 0 < \rho_{k,l} := & 1 + \tau^2 \left(\Phi^{-1} \left(\frac{1 + \tau + p}{2} \right) + \epsilon \right)^2 (1 + \delta_{2k+s-1})^2 \mu_{k,l}^2 \\ & - 2c_k \sqrt{\frac{2}{\pi}} \left(\tau - \frac{|T_1^{k,l}|}{m} \right) (1 - \delta_{2k+s-1}) \mu_{k,l} < \frac{1}{3}. \end{aligned} \quad (2.7)$$

Here $c_k = (2 - 2p)(1 - \delta_{2k+s-1}) - (1 + \delta_{2k+s-1})$, $T_1^{k,l} = T \cap \Gamma^{k,l}$, $\Gamma^{k,l} = \{i : |b_i - (\mathbf{A}\mathbf{u}^{k,l})_i| \leq \theta_\tau(|\mathbf{b} - \mathbf{A}\mathbf{u}^{k,l}|)\}$, and ϵ is a small constant. Then the k -th iterate \mathbf{x}^k satisfies:

$$\|\mathbf{x}_0 - \mathbf{x}^k\|_2^2 \leq \left(\frac{(\rho_k)^{L+1}(1 - 3\rho_k) + 2\rho_k}{1 - \rho_k} \right) \|\mathbf{x}_0 - \mathbf{x}^{k-1}\|_2^2, \quad (2.8)$$

where $\mathbf{u}^{k,L+1} := \mathbf{x}^k$, $\mathbf{u}^{k,0} := \mathbf{x}^{k-1}$, $\rho_k = \max_{l=0}^L \rho_{k,l}$, and $k \geq s$.

Then, we show a corollary which displays the convergence of FHTP₁ algorithm.

Corollary 2.3. *Let $\mathbf{x}_0 \in \mathbb{R}^n$ be s -sparse and $\mathbf{b} = \mathbf{A}\mathbf{x}_0 + \boldsymbol{\eta}$ for some $\boldsymbol{\eta}$ with $T = \text{supp}(\boldsymbol{\eta})$ and $|T| = pm$. Assume that the matrix \mathbf{A} satisfies RIP_1 with RIC_1 satisfying $0 < \delta_{3s} < 0.25$. Suppose that the fraction of outliers p satisfies $p < \frac{1}{2} - \frac{\delta_{3s}}{1-\delta_{3s}}$. Let (\mathbf{x}^k) be the sequence generated by FHTP₁ and adaptive step size satisfying the same form as Theorem 2.2 (replacing δ_{2k+s-1} with δ_{3s}). Then*

$$\|\mathbf{x}_0 - \mathbf{x}^k\|_2^2 \leq \left(\frac{(\rho_k)^{L+1}(1 - 3\rho_k) + 2\rho_k}{1 - \rho_k} \right) \|\mathbf{x}_0 - \mathbf{x}^{k-1}\|_2^2, \quad (2.9)$$

where $\rho_k = \max_{l=0}^L \rho_{k,l}$, and $c_k = (2 - 2p)(1 - \delta_{3s}) - (1 + \delta_{3s})$. Moreover, we obtain

$$\|\mathbf{x}_0 - \mathbf{x}^k\|_2 \leq \rho^k \|\mathbf{x}_0 - \mathbf{x}^0\|_2 \quad (2.10)$$

with $\rho := \max_k \sqrt{\frac{(\rho_k)^{L+1}(1 - 3\rho_k) + 2\rho_k}{1 - \rho_k}}$. With the initialization $\mathbf{x}^0 = \mathbf{0}$, we can reconstruct an s -sparse signal \mathbf{x}_0 with an accuracy of $\|\mathbf{x}^{k^*} - \mathbf{x}_0\|_2 \leq \varepsilon$ after

$$k^* = \left\lceil \log_{\frac{1}{\rho}} \frac{\|\mathbf{x}_0\|_2}{\varepsilon} \right\rceil$$

iterations.

Note: FHTP₁ uses fixed sparsity s , so the RIP_1 order is $3s$.

Next, we give a remark which checks the sufficient condition (2.7) in Theorem 2.2.

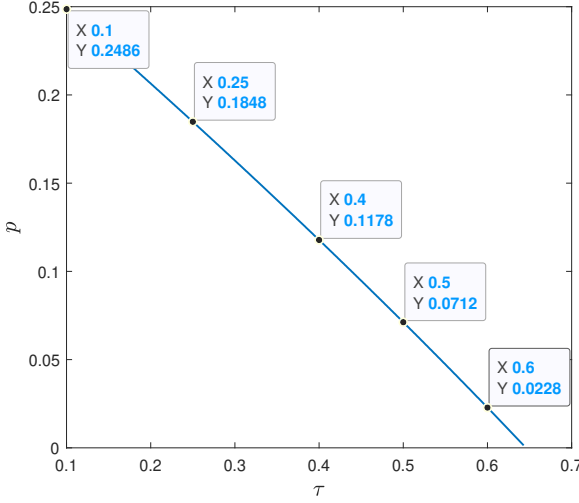


Figure 1: The maximum value of the outliers proportion p under general case.

Remark 2.4. It seems that the sufficient condition (2.7) is complex and strict. In fact, this condition can be met. Notice that the sufficient condition (2.7) provides a quadratic inequality $ax^2 - bx + c < 0$ for $x = \mu_{k,l}$ with $a = \tau^2 \left(\Phi^{-1} \left(\frac{1+\tau+p}{2} \right) + \epsilon \right)^2 (1 + \delta_{2k+s-1})^2$, $b = 2c_k \sqrt{\frac{2}{\pi}} \left(\tau - \frac{|T_1^{k,l}|}{m} \right) (1 - \delta_{2k+s-1})$ and $c = 2/3$. For this quadratic inequality to have real solutions, it is necessary to ensure that $b^2 - 4ac > 0$; when this condition holds, the inequality has solutions given by $(b - \sqrt{b^2 - 4ac})/2a < \mu_{k,l} < (b + \sqrt{b^2 - 4ac})/2a$. We set $\epsilon = 0.001$, $\delta_{2k+s-1} = 0.01$, $|T_1^{k,l}|/m = 0.001$, $\tau = 0.1 : 0.001 : 0.7$, $p = 0.001 : 0.0001 : 0.5$.

It follows from Theorem 2.2 that $\|\mathbf{x}_0 - \mathbf{u}^{k,L+1}\|_2^2 = \|\mathbf{x}_0 - \mathbf{x}^k\|_2^2 \leq \rho^k \|\mathbf{x}_0 - \mathbf{x}^0\|_2^2 \rightarrow 0$. Therefore the ratio $|T_1^{k,l}|/m$ tends to zero with the increase of iteration number k . So we can take $|T_1^{k,l}|/m \leq 0.001$. The selectable range for the outlier proportion p is shown in Figure 1. Especially,

- (i) when $\tau = 0.5, p = 0.05$, we can take $1.3695 < \mu_{k,l} < 3.3362$ to make this condition (2.7) true;
- (ii) we can set $\tau = 0.1, p = 0.2$, then we can find that when $8.7136 < \mu_{k,l} < 50.2541$, the condition (2.7) is satisfied.

2.2.3 Exact Recovery for Structured Sparse Signals

Theorem 2.5. Consider an s -sparse vector $\mathbf{x}_0 \in \mathbb{R}^n$ satisfying $x_1^* \leq \lambda x_s^*$ ($\lambda \geq 1$, e.g., ‘flat’ signals with $\lambda = 1$). Assume that the sensing matrix \mathbf{A} is an $m \times n$ matrix whose entries are independently and identically distributed (i.i.d.) Gaussian random variables, i.e., $a_{ij} \sim \mathcal{N}(0, \frac{1}{m^2})$ with $m \geq c'_1 s \log n$. Let the measurements $\mathbf{b} = \mathbf{Ax}_0 + \boldsymbol{\eta}$, where $\boldsymbol{\eta}$ is a vector of outliers with support T and cardinality $|T| = pm$. Assume that RIC_1 satisfies $0 < \delta_s < 0.25$ and the fraction of outliers p satisfies $p < \frac{1}{2} - \frac{\delta_s}{1 - \delta_s}$. The adaptive step size $t_{k,0}$ for the GFHTP₁ algorithm is defined as $\mu_{k,0} \sqrt{\frac{\pi}{2}} \|\mathbf{b} - \mathbf{Ax}^{k-1}\|_2 \odot (\mathbb{I}_{\{|b_i - (\mathbf{Ax}^{k-1})_i| \leq \theta_\tau (|\mathbf{b} - \mathbf{Ax}^{k-1}|)\}})_{i=1}^m \|_1$, where $\mu_{k,0}$ satisfies

$$\begin{aligned}
0 < \beta'_k := & 1 + 2\tau^2 \left(\Phi^{-1} \left(\frac{1+\tau+p}{2} \right) + \epsilon \right)^2 (1 + \delta_s)^2 \mu_{k,0}^2 \\
& - 2c \sqrt{\frac{2}{\pi}} \left(\tau - \frac{|T_1^{k,0}|}{m} \right) (1 - \delta_s) \mu_{k,0} < \frac{1}{2 + \lambda^2},
\end{aligned} \tag{2.11}$$

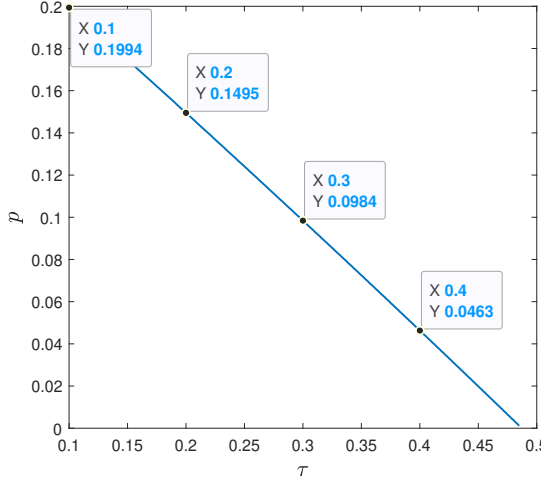


Figure 2: The maximum value of the outliers proportion p under ‘flat’ vector.

and $T_1^{k,0} = T \cap \Gamma^{k,0}$, $\Gamma^{k,0} = \{i : |b_i - (\mathbf{A}\mathbf{x}^{k-1})_i| \leq \theta_\tau(|\mathbf{b} - \mathbf{A}\mathbf{x}^{k-1}|)\}$, c is defined as $(2 - 2p)(1 - \delta_s) - (1 + \delta_s)$ and $k \leq s + 1$. Under these conditions, with a probability of at least $1 - n^{-c''}$, the sequence of supports (S^k) and the sequence of estimates (\mathbf{x}^k) generated by GFHTP₁ will satisfy the following results at iteration s :

$$S^s = \text{supp}(\mathbf{x}_0), \quad \mathbf{x}^s = \mathbf{x}_0.$$

Remark 2.6. In fact, the condition (2.11) of Theorem 2.5 can be met. We consider the following special case: assume that $\lambda = 1$ and $\epsilon = 0.001, \delta_s = 0.01, |T_1^{k,l}|/m = 0.001, \tau = 0.1 : 0.001 : 0.5, p = 0.001 : 0.0001 : 0.5$. The selectable range for the outliers proportion p is shown in Figure 2. Especially,

- (i) when $\tau = 0.4, p = 0.01$, we can take $1.4444 < \mu_{k,0} < 4.8518$ to make this condition (2.11) true;
- (ii) we can set $\tau = 0.1, p = 0.15$, then we can find that when $7.4256 < \mu_{k,0} < 43.0710$, the condition (2.11) is satisfied.

Lastly, we give a remark which provides the comparison with the state-of-the-art methods.

Remark 2.7. (i) In [21], the theoretical findings presented are not directly suitable for scenarios with a significant presence of outliers, given that $\|\boldsymbol{\eta}\|_1$ is substantial. Furthermore, the sparsity level s is frequently unknown in real-world applications. Our work provides a theoretical analysis of the GFHTP₁ algorithm, addressing the limitation identified in [21]. We also notice that Li et al. [21] choose an adaptive step size $t_k = \mu \|\mathbf{b} - \mathbf{A}\mathbf{x}^k\|_1$ for a fixed constant μ , which is effective primarily for bounded noise. While our truncated adaptive step size $t_{k,l} = \mu_{k,l} \sqrt{\frac{\pi}{2}} \|(\mathbf{b} - \mathbf{A}\mathbf{u}^{k,l}) \odot (\mathbb{I}_{\{|b_i - (\mathbf{A}\mathbf{u}^{k,l})_i| \leq \theta_\tau(|\mathbf{b} - \mathbf{A}\mathbf{u}^{k,l}|)\}})_{i=1}^m\|_1$ is designed to handle outliers more effectively.

- (ii) In contrast to the step size selection in the PSGD algorithm proposed by Xu et al. [31], which hinges on the actual signal characteristics, this dependency is impractical. Therefore, our approach determines the step size independently of the signal itself. Furthermore, we also design a high-efficiency stopping criterion $\|(\mathbf{b} - \mathbf{A}\mathbf{x}^{k+1}) \odot (\mathbb{I}_{\{|b_i - (\mathbf{A}\mathbf{x}^{k+1})_i| \leq \theta_\tau(|\mathbf{b} - \mathbf{A}\mathbf{x}^{k+1}|)\}})_{i=1}^m\|_1 \leq \epsilon_{\text{outer}}$, which ensures fast and high-precision convergence, thereby addressing the lack of a suitable stopping criterion in [31].

3 The Roadmap and Keystone of Our Proofs

In this section, we present the proof strategies for Theorems 2.2 and 2.5. This section serves as the foundation for the subsequent convergence analysis in the Appendices.

3.1 The Roadmap and Keystone of the Proof of Theorem 2.2

The proof strategy of Theorem 2.2 can be summarized in the following two key steps:

(a) Contraction of the inner iteration: The central step is to establish the following inequality:

$$\|\mathbf{x}_0 - \mathbf{u}^{k,l+1}\|_2^2 \leq \rho_{k,l} \|\mathbf{x}_0 - \mathbf{u}^{k,l}\|_2^2 + 2\rho_{k,0} \|\mathbf{x}_0 - \mathbf{x}^{k-1}\|_2^2,$$

where $\rho_{k,l} = 1 + \tau^2(\Phi^{-1} + \epsilon)^2(1 + \delta_{2k+s-1})^2\mu_{k,l}^2 - 2c_k\sqrt{\frac{2}{\pi}}\left(\tau - \frac{|T_1^{k,l}|}{m}\right)(1 - \delta_{2k+s-1})\mu_{k,l}$ with $\Phi^{-1} := \Phi^{-1}(\frac{1+\tau+p}{2})$, and $T_1^{k,l} = T \cap \Gamma^{k,l}$ with $\Gamma^{k,l} = \{i : |b_i - (\mathbf{A}\mathbf{u}^{k,l})_i| \leq \theta_\tau(|\mathbf{b} - \mathbf{A}\mathbf{u}^{k,l}|)\}$.

(b) Convergence of the iteration: By induction, we prove

$$\|\mathbf{x}_0 - \mathbf{x}^k\|_2^2 = \|\mathbf{x}_0 - \mathbf{u}^{k,L+1}\|_2^2 \leq \left(\frac{\rho_k^{L+1}(1 - 3\rho_k) + 2\rho_k}{1 - \rho_k}\right) \|\mathbf{x}_0 - \mathbf{x}^{k-1}\|_2^2, \quad (3.1)$$

where $\rho_k = \max_l \rho_{k,l}$ and $k \geq s$.

Notice that in Step (a), we need to show the contraction property of the inner iteration. To complete the key step, we need two key propositions. The first one gives the upper and lower bounds for the quantity $\|(\mathbf{b} - \mathbf{A}\mathbf{x}) \odot (\mathbb{I}_{\{|b_i - (\mathbf{A}\mathbf{x})_i| \leq \theta_\tau(|\mathbf{b} - \mathbf{A}\mathbf{x}|)\}})_{i=1}^m\|_1$.

Proposition 3.1. *For fixed $\epsilon \in (0, 1)$, a matrix $\mathbf{A} = [\mathbf{a}_1, \dots, \mathbf{a}_m]^\top \in \mathbb{R}^{m \times n}$ ($m \ll n$) with i.i.d. Gaussian entries, $a_{ij} \sim \mathcal{N}(0, \frac{1}{m^2})$.*

(i) *If $m \geq d_0(\epsilon^{-2} \log(\epsilon^{-1}))(s+k) \log n$ for some large enough constant d_0 , then with probability at least $1 - d_1 \exp(-d_2 m \epsilon^2) - \frac{1}{n}$, where d_1 and d_2 are some constants, we have for all signals $\mathbf{x} \in \mathbb{R}^n$ with $\|\mathbf{x}\|_0 = s+k$ ($k \in \mathbb{Z}^+$):*

$$m\theta_\tau(|\mathbf{A}\mathbf{x}|) \in \left[\Phi^{-1}\left(\frac{1+\tau}{2}\right) - \epsilon, \Phi^{-1}\left(\frac{1+\tau}{2}\right) + \epsilon\right] \|\mathbf{x}\|_2. \quad (3.2)$$

(ii) *For the model (1.1) contaminated by outliers $\boldsymbol{\eta}$, with $T = \text{supp}(\boldsymbol{\eta})$ and $p = \frac{|T|}{m}$, we derive the following upper bound with high probability:*

$$\|(\mathbf{b} - \mathbf{A}\mathbf{x}) \odot (\mathbb{I}_{\{|b_i - (\mathbf{A}\mathbf{x})_i| \leq \theta_\tau(|\mathbf{b} - \mathbf{A}\mathbf{x}|)\}})_{i=1}^m\|_1 \leq \tau \left(\Phi^{-1}\left(\frac{1+\tau+p}{2}\right) + \epsilon\right) \|\mathbf{x} - \mathbf{x}_0\|_2,$$

and the following lower bound:

$$\|(\mathbf{b} - \mathbf{A}\mathbf{x}) \odot (\mathbb{I}_{\{|b_i - (\mathbf{A}\mathbf{x})_i| \leq \theta_\tau(|\mathbf{b} - \mathbf{A}\mathbf{x}|)\}})_{i=1}^m\|_1 \geq \left(\tau - \frac{|T_1|}{m}\right) \sqrt{\frac{2}{\pi}}(1 - \delta_{s+l}) \|\mathbf{x} - \mathbf{x}_0\|_2,$$

where $T_1 = T \cap \Gamma$ with $\Gamma = \{i : |b_i - (\mathbf{A}\mathbf{x})_i| \leq \theta_\tau(|\mathbf{b} - \mathbf{A}\mathbf{x}|)\}$, $\|\mathbf{x}_0\|_0 = s$, and $\|\mathbf{x}\|_0 = \ell$.

The second proposition implies that the updated vector $\mathbf{u}^{k,l} + t_{k,l}\mathbf{A}^\top \text{sign}(\mathbf{b} - \mathbf{A}\mathbf{u}^{k,l})$ by the subgradient descent method is close to the true signal \mathbf{x}_0 .

Proposition 3.2. *Let S, S^{k-1} and S^k denote the supports of $\mathbf{x}_0, \mathbf{x}^{k-1}$ (or $\mathbf{u}^{k,0}$), and $\mathbf{u}^{k,l}$ for $1 \leq l \leq L+1$, respectively. Denote the index set*

$$\Lambda^k := S \cup S^{k-1} \cup S^k.$$

Then we have

$$\|[\mathbf{x}_0 - \mathbf{u}^{k,l} - t_{k,l}\mathbf{A}^\top \text{sign}(\mathbf{b} - \mathbf{A}\mathbf{u}^{k,l})]_{\Lambda^k}\|_2^2 \leq \rho_{k,l} \|\mathbf{x}_0 - \mathbf{u}^{k,l}\|_2^2, \quad (3.3)$$

where $\rho_{k,l} = 1 + \tau^2 \left(\Phi^{-1}\left(\frac{1+\tau+p}{2}\right) + \epsilon\right)^2 (1 + \delta_{2k+s-1})^2 \mu_{k,l}^2 - 2c_k \sqrt{\frac{2}{\pi}} \left(\tau - \frac{|T_1^{k,l}|}{m}\right) (1 - \delta_{2k+s-1}) \mu_{k,l}$.

3.2 The Roadmap and Keystone of the Proof of Theorem 2.5

We first list the outline of the proof of Theorem 2.5. Define the set S as the support of \mathbf{x}_0 and introduce two random variables, ζ_k and ξ_k , for $k \in [[s]]$, as follows:

$$\begin{aligned}\zeta_k &:= [(\mathbf{x}^{k-1} + t_{k,0} \mathbf{A}^\top \text{sign}(\mathbf{b} - \mathbf{A}\mathbf{x}^{k-1}))_S]_k^*, \\ \xi_k &:= [(\mathbf{x}^{k-1} + t_{k,0} \mathbf{A}^\top \text{sign}(\mathbf{b} - \mathbf{A}\mathbf{x}^{k-1}))_{S^c}]_1^*.\end{aligned}$$

Here, ζ_k represents the k -th largest value of the elements in the subset S of $|(\mathbf{x}^{k-1} + t_{k,0} \mathbf{A}^\top \text{sign}(\mathbf{b} - \mathbf{A}\mathbf{x}^{k-1}))_j|$, while ξ_k denotes the largest value of the elements in the complementary subset S^c . Our outline can be summarized in the following three key steps:

- (a') Establish that with high probability, $S^k \subseteq S$ for each $k \in [[s]]$. This is implied by the condition $\zeta_k > \xi_k$ for all $k \in [[s]]$.
- (b') Show that the event $\mathcal{E} = \{(\exists k \in [[s]] : \xi_k \geq \zeta_k \text{ and } (\zeta_{k-1} > \xi_{k-1}, \dots, \zeta_1 > \xi_1))\}$ occurs with small probability. In particular, we obtain $\zeta_k > \xi_k$ for all $k \in [[s]]$ with high probability, which implies that $S^s = S$.
- (c') Obtain the conclusion $\mathbf{x}^s = \mathbf{x}_0$, due to the contradiction that $\|\mathbf{x}_0 - \mathbf{x}^s\|_2^2 < \|\mathbf{x}_0 - \mathbf{x}^s\|_2^2$.

In order to prove the key step (a'), we need the following key proposition.

Proposition 3.3. *The event $\mathcal{F} = \{\xi_k \geq \zeta_k, k \in [[s]]\}$ occurs with probability at most*

$$2(n-s) \exp\left(-\frac{\gamma_k^2 m}{6s}\right),$$

where $\gamma_k = \frac{\sqrt{\frac{2}{\pi}}}{\mu_{k,0}\tau(\Phi^{-1}(\frac{1+\tau+p}{2})+\epsilon)} \left(\frac{\sqrt{1-2\beta'_k}}{\lambda} - \sqrt{\beta_k} \right)$, $\beta_k = 1 + \tau^2(\Phi^{-1}(\frac{1+\tau+p}{2}) + \epsilon)^2(1 + \delta_s)^2\mu_{k,0}^2 - 2c\sqrt{\frac{2}{\pi}}\left(\tau - \frac{|T_1^{k,0}|}{m}\right)(1 - \delta_s)\mu_{k,0}$, and β'_k is denoted by Theorem 2.5.

4 Numerical Experiments

In this section, we embark on numerical experiments to demonstrate the efficacy of the GFHTP₁ algorithm in tackling sparse signal recovery challenges, particularly in the presence of outliers. Our synthetic and real-world data experiments validate the robustness and efficiency of GFHTP₁ in identifying and mitigating the impact of outliers, aligning with the theoretical guarantees presented in Theorems 2.2 and 2.5.

4.1 Experiments Settings

We commence by outlining the foundational parameters for our experiments. Firstly, the sensing matrix $\mathbf{A} \in \mathbb{R}^{m \times n}$ is constructed with entries drawn from the i.i.d. Gaussian distribution $\mathcal{N}(0, \frac{1}{m^2})$. Here and following, we set $m = 1000, n = 5000$. For the purpose of this section, we generate two types of s -sparse underlying signal $\mathbf{x}_0 \in \mathbb{R}^n$, referred to as

- (i) the Gaussian signal with its non-zero entries being i.i.d. standard Gaussian variables;
- (ii) the ‘flat’ signal with $(\mathbf{x}_0)_j = 1$ for $j \in S$, where $S = \text{supp}(\mathbf{x}_0)$ and $|S| = s$.

To introduce outliers, we first identify pm random positions, where the ratio p represents the proportion of non-zero elements in η . We consider two types of corruptions:

- (i) Gaussian outliers: we populate these positions with i.i.d. Gaussian entries with mean zero and variance $\sigma_{\text{outliers}}^2$, while the rest are set to zero;

- (ii) Uniform outliers: we populate these positions with uniform distribution $\mathcal{U}(-u_{\text{outliers}}, u_{\text{outliers}})$, while the rest are set to zero.

The measurement vector \mathbf{b} is constructed in accordance with Equation (1.1), with $b_i = \mathbf{a}_i^\top \mathbf{x}_0 + \boldsymbol{\eta}_i$ for $i \in T$ and $b_i = \mathbf{a}_i^\top \mathbf{x}_0$ for $i \in T^c$, where $T = \text{supp}(\boldsymbol{\eta})$ denotes the support of the outliers $\boldsymbol{\eta}$.

Lastly, we mark $\hat{\mathbf{x}}$ as the recovered signal. We evaluate the numerical performance using the following metric for all algorithms:

- (i) Relative error (RelErr): $\text{RelErr}(\hat{\mathbf{x}}, \mathbf{x}_0) = \|\hat{\mathbf{x}} - \mathbf{x}_0\|_2 / \|\mathbf{x}_0\|_2$;
- (ii) Success rate (SR): the success rate of recovery in 100 trials, and a successful reconstruction is declared when $\text{RelErr}(\hat{\mathbf{x}}, \mathbf{x}_0) \leq \epsilon$ with $\epsilon = 10^{-4}$.

All settings, unless otherwise specified, shall be selected as above. Each experiment is replicated 100 times to ensure statistical significance and all results report the mean value over 100 independent trials.

4.2 The Performance of Our Algorithms

a) The Chooses of Step Sizes $\mu_{k,l}$

Firstly, we test the performance of different step sizes $\mu_{k,l}$ in Remark 2.4. Here we take the gaussian outliers with the parameter $\sigma_{\text{outliers}} = 10$, the quantile $\tau = 0.5$, and $s = 5, 10, 15$. The numbers of iterations for the outer and inner iterations are $\text{MaxIt} = 30$ and $L = 10$ respectively. Figure 3 shows the performance of the algorithm in terms of relative error, average CPU time, and the sparsity of the recovered signal when the sparsity is 5, 10, and 15, the outliers ratio ranges from 0.05 to 0.5, and different $\mu_{k,l}$ values are selected. Notably, our theoretical result requires that $\mu_{k,l}$ to be fixed within the interval $(1.3695, 3.3362)$ when $\tau = 0.5, p = 0.05$. However from Figure 3, we can see that our GFHTP₁ exhibits superior performance when the step size is $\mu_{k,l} = 4, 6, 8$. Especially, when $\mu_{k,l} = 1$, the relative error is small, however the sparsity of the recovered signal is not exact. This discrepancy between the theoretical result and empirical effectiveness highlights an important direction for future work. Motivated by these experimental findings, we adopt $\mu_{k,l} = 6$ for all subsequent experiments.

b) The Choices of Inner Iterations L

Next, we explore the performance of different inner iterations L . Some fundamental settings are $\sigma_{\text{outliers}} = 10$, the quantile $\tau = 0.5$, $\mu_{k,l} = 6$, and $s = 5, 10, 15$. The number of iterations for the outer iteration is $\text{MaxIt} = 30$. We show this result in Figure 4. From Figure 4, we can know that as L increases, the relative error decreases, but the time increases accordingly. Meanwhile, the sparsity of recovered signal is inaccurate when $L = 1$. Therefore, considering both time and accuracy, we choose $L = 10$.

c) Performance of Different Quantiles τ

Then, we consider the result of different quantiles τ . Some fundamental settings are $\sigma_{\text{outliers}} = 10, u_{\text{outliers}} = 100, s = 5, \mu_{k,l} = 6, L = 10$. The number of iterations for the outer iteration is $\text{MaxIt} = 30$. Figure 5 shows the performance of the algorithm in terms of relative error when the sparsity is 5, the outliers ratio ranges from 0.05 to 0.55, and different τ values are selected. From Figure 5, when the quantile τ is 0.35, it can be seen that a more accurate recovery can be achieved even when the proportion of outliers is 0.55. When the quantile τ is 0.5, the effect is very good except when the proportion of outliers is 0.55. However, when the quantile τ is 0.8, the effect is not satisfactory even when the proportion of outliers is 0.2, that is, $\tau \leq 1 - p$. Therefore, in the subsequent experiments, we choose a more general quantile, namely the median.

Similarly, we can get same results using the FHTP₁ algorithm. Thus, we set $\mu_{k,l} = 6, L = 10$.

Then, our result is shown in Figure 6, thus implying that the GFHTP₁ with adaptive step sizes can exactly recover the underlying sparse signal \mathbf{x}_0 when the sparsity of the real signal is unknown. Especially, we assume that the sparsity of the original signal is known, we can show the performance of FHTP₁ algorithm in Figure 7. Compared with Figure 6, we can see that FHTP₁

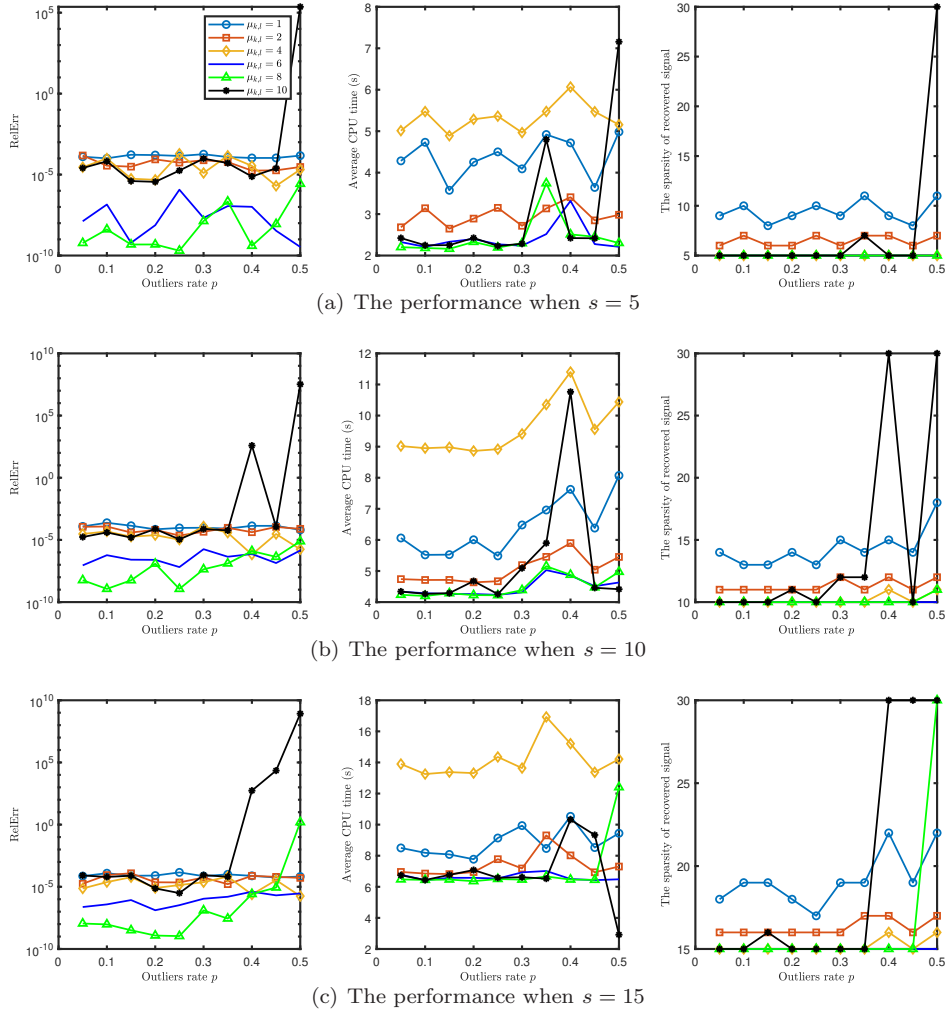


Figure 3: Relative error, average CPU time, the sparsity of the recovered signal for the GFHTP₁ algorithm using Gaussian outliers.

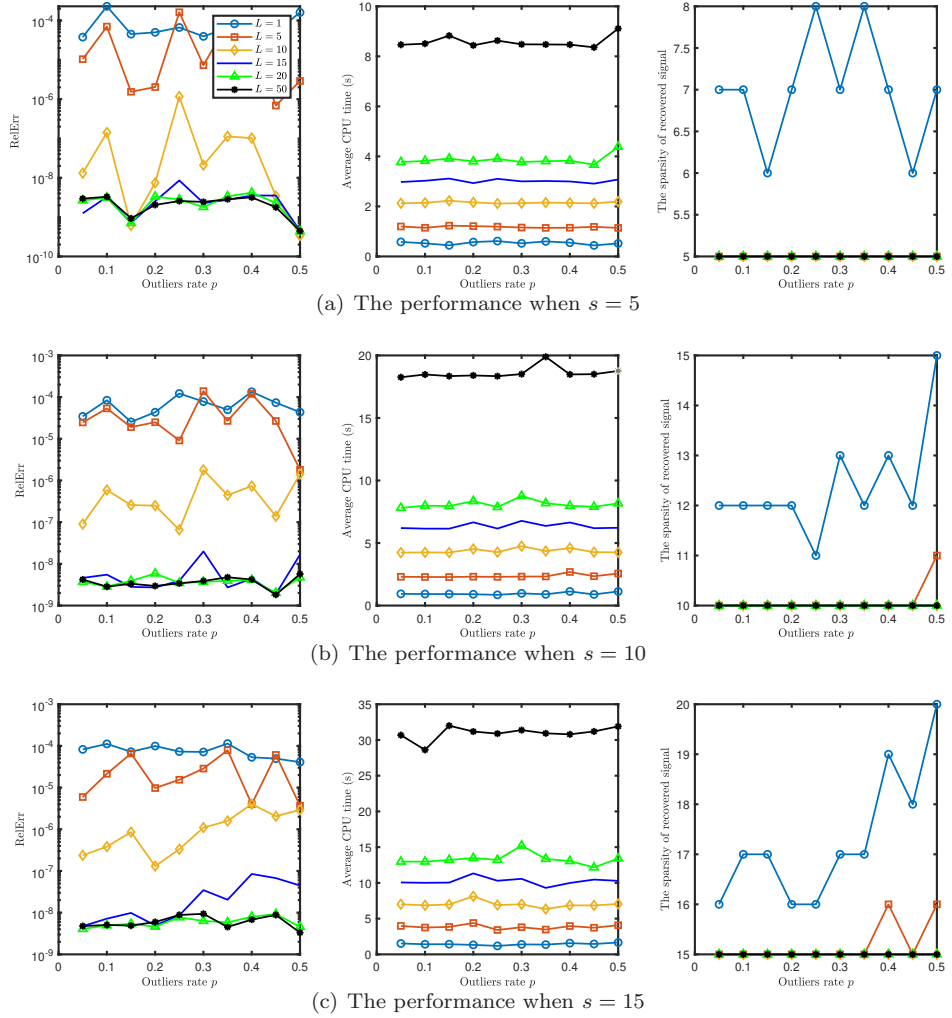


Figure 4: Numerical performance for the GFHTP₁ algorithm using Gaussian outliers when various L .

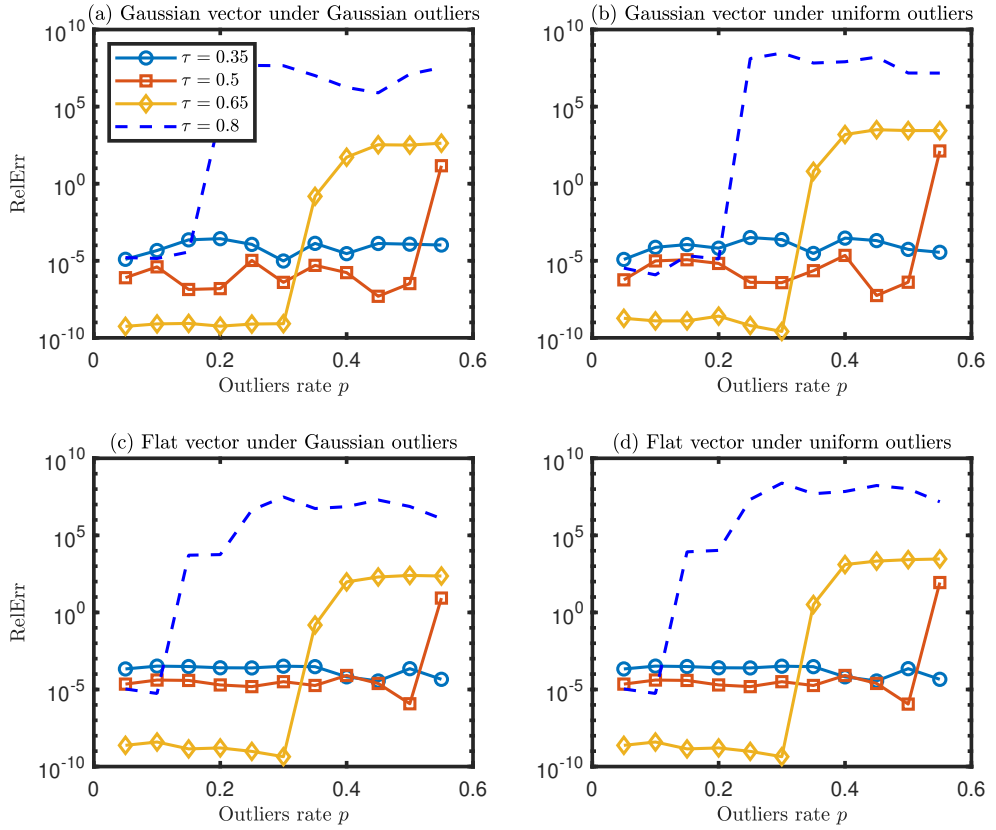


Figure 5: Numerical performance for the GFHTP₁ algorithm when various τ .

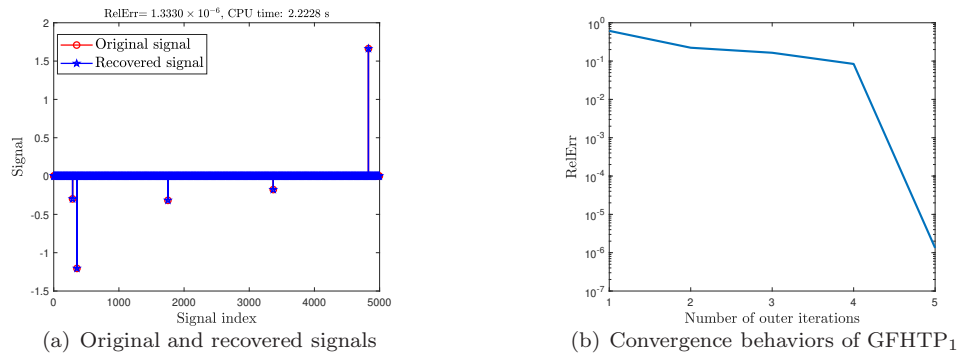


Figure 6: Performance of our proposed GFHTP₁ algorithm for Gaussian vector and Gaussian outliers with $\sigma_{\text{outliers}} = 10$ and $p = 0.2$.

is faster with comparable result than GFHTP₁. However, the sparsity is usually unknown and inaccurate sparsity can have a huge impact on the recovery effect. Therefore, studying GFHTP₁ makes sense, although it takes more time.

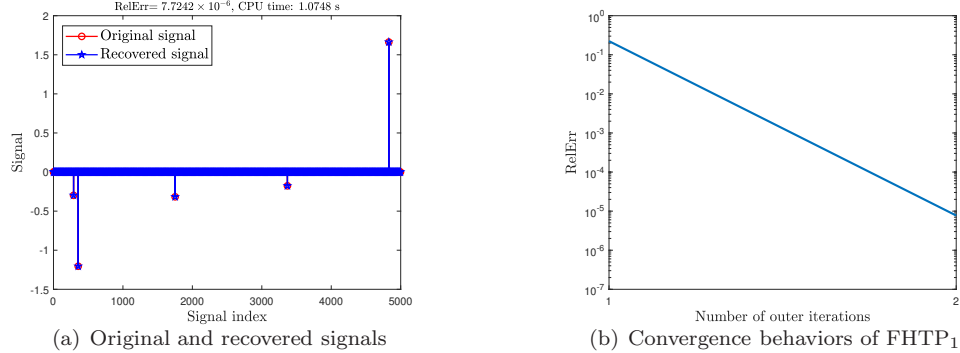


Figure 7: Performance of our proposed FHTP₁ algorithm for Gaussian vector and Gaussian outliers with $\sigma_{\text{outliers}} = 10$ and $p = 0.2$.

Lastly, we verify the effect of Theorem 2.5. We choose the ‘flat’ vector as original signal. Some fundamental settings are $\sigma_{\text{outliers}} = 10$, $s = 5$, $\mu_{k,l} = 6$, $L = 10$. The result is shown in Figure 8. From Figure 8, we can see that $S^1, S^2, S^3, S^4, S^5 \subseteq S$ and $S^5 = \text{supp}(\mathbf{x}_0)$. It can be approximately regarded as $\mathbf{x}^5 = \mathbf{x}_0$. Therefore, Theorem 2.5 has been verified.

4.3 Comparison with Other Algorithms

In this section, we first compare the several methods with Gaussian vector whose s nonzero entries are independent standard normal random variables in no outliers case. We set $p = 0$, $L = 10$. We give the fundamental settings of the other existing algorithms in sparse signal recovery: PSGD (with real sparsity s), PSGD² (with the sparsity level as $2s$), AIHT (with real sparsity s), AIHT² (with the sparsity level as $2s$). The PSGD and PSGD² algorithms utilize the step size $\mu_k = 0.8 \times 0.95^k$. And we used the criterion $\text{RelErr}(\mathbf{x}^{k+1}, \mathbf{x}^k) \leq 10^{-8}$ or the maximum iteration number 1000 for PSGD, PSGD², AIHT and AIHT². We present here a comparison between PSGD, PSGD², AIHT, AIHT² and GFHTP₁, FHTP₁ in terms of successful recovery. The result is shown in Figure 9. From Figure 9, we can find that our algorithm outperforms the others. Our algorithm needs more CPU time because it takes too much time to search for true sparsity. Thus our algorithm is robust for the absence of outliers.

Next, we present the results for outliers case. For AIHT algorithm, we set $p = 0.05, 0.1, \sigma_{\text{outliers}} = 10, 100$, the results are shown in Figure 10. It is easy to see that the two methods are invalid for outliers case. So we compare the performance of the remaining algorithms. We set $s = 5, 10, \sigma_{\text{outliers}} = 10$. For different outliers rate $p = 0.05i (i = 1, \dots, 10)$, the success rates and average CPU time are shown in Tables 1 and 2. We can see that our algorithm is also effective when the outliers rate is high. And our algorithm takes less time and works better than PSGD.

4.4 Test on Real Data

In this subsection, we validate the effectiveness of our proposed algorithms in the context of image restoration. Specially, the MNIST test dataset-comprising 10000 handwritten digit images-is adopted for experimental evaluation. Each image in this dataset has a resolution of 28×28 pixels, with a black background and white foreground content. Owing to the limited proportion of white areas, the images can be considered sparse. Each image is vectorized into a column vector as the sparse vector \mathbf{x}_0 . The observation vector \mathbf{b} is obtained through $\mathbf{b} = \mathbf{Ax}_0 + \boldsymbol{\eta}$ with the outliers $\boldsymbol{\eta}$.

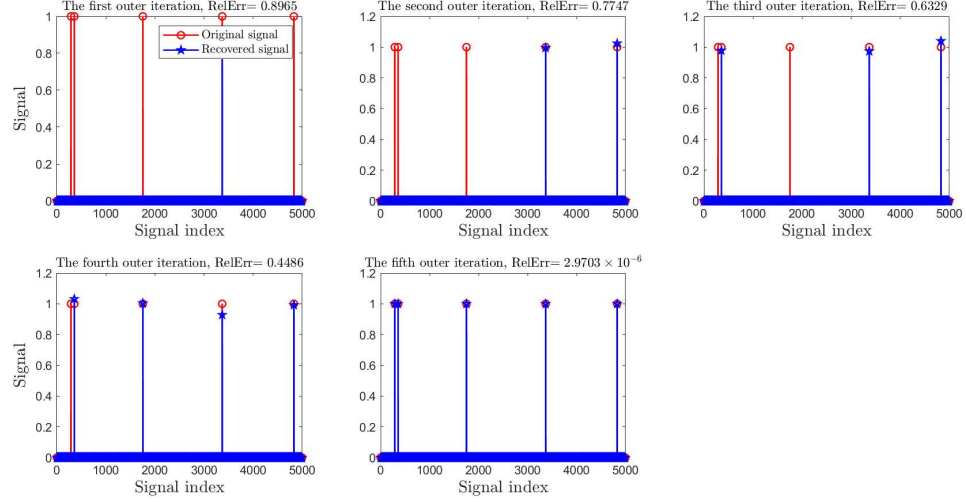


Figure 8: Numerical performance for the GFHTP₁ algorithm under the ‘flat’ vector case.

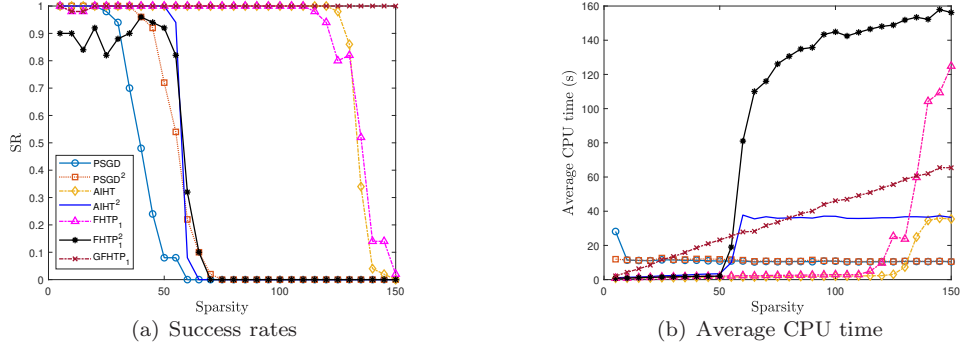


Figure 9: Rates of successful recoveries and average CPU times for PSGD, PSGD², AIHT, AIHT² and GFHTP₁ using Gaussian measurements.

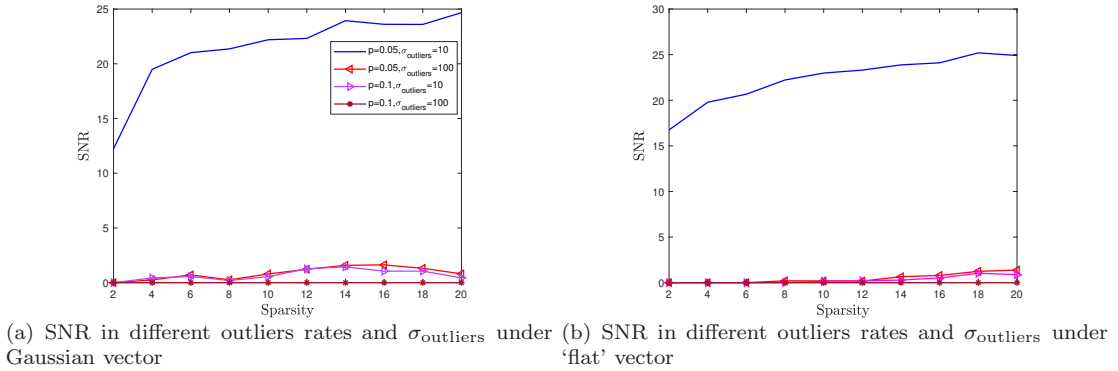


Figure 10: SNR for AIHT using Gaussian vector and ‘flat’ vector in outliers case.

Table 1: The success rates and average CPU time (s) in different outliers rates and different sparsity by different algorithms under Gaussian vector.

Sparsity	$s = 5$			$s = 10$		
	PSGD	FHTP ₁	GFHTP ₁	PSGD	FHTP ₁	GFHTP ₁
0.05	1,12.2750	1,0.8126	1,2.2274	1,11.9584	0.99,1.0992	0.99,4.5080
0.10	1,11.9099	1,0.8284	1,2.1784	1,11.9567	1,1.1192	1,4.4967
0.15	1,11.8507	1,0.8209	1,2.1786	1,11.9303	0.99,1.1094	0.99,4.4813
0.20	1,11.8399	1,0.8279	1,2.1924	0.98,11.8560	1,1.1960	1,4.5566
0.25	1,11.8435	1,0.8766	1,2.1838	0.93,11.7049	0.99,1.1840	0.99,4.5112
0.30	1,11.8230	1,0.8913	1,2.1888	0.86,11.2739	1,1.2191	1,4.4501
0.35	0.98,11.5808	1,0.9036	1,2.1803	0.76,11.0234	1,1.3530	1,4.4405
0.40	0.96,11.5065	1,0.9359	1,2.1820	0.47,10.3424	1,1.3996	1,4.4441
0.45	0.72,10.8374	1,1.0428	1,2.1862	0.25,9.8564	1,1.4571	1,4.4539
0.50	0.71,10.7115	1,1.0163	1,2.1792	0.05,9.6208	1,1.5884	1,4.4620

Table 2: The success rates and average CPU time (s) in different outliers rates and different sparsity by different algorithms under ‘flat’ vector.

Sparsity	$s = 5$			$s = 10$		
	PSGD	FHTP ₁	GFHTP ₁	PSGD	FHTP ₁	GFHTP ₁
0.05	1,12.0905	1,0.4454	1,2.2258	1,12.5671	1, 0.4764	0.99,4.7804
0.10	1,11.4555	1,0.4230	1,2.1067	1,11.9900	1, 0.4513	1,4.5219
0.15	1,11.4388	1,0.4247	1,2.1157	1,11.4821	1, 0.4349	1,4.3494
0.20	1,11.3687	1,0.4214	1,2.1105	1,11.4300	1, 0.4820	1,4.3460
0.25	1,11.3648	1,0.4233	1,2.1141	1,11.3538	0.99, 0.4893	1,4.3378
0.30	1,11.2867	1,0.4222	1,2.1093	0.91,11.0272	1, 0.6082	1,4.3319
0.35	1,11.2749	1,0.4233	1,2.1129	0.80,10.7377	1, 0.6797	1,4.3307
0.40	1,11.2021	1,0.4270	1,2.1134	0.26,9.3547	1, 0.8074	1,4.3360
0.45	0.94,12.0457	1,0.5136	1,2.3220	0.09,9.2260	1, 0.8541	1,4.3486
0.50	0.82,10.9066	1,0.5122	1,2.1932	0,9.2853	1, 0.9455	1,4.3274

Subsequently, the different algorithms are applied to reconstruct the original sparse signal \mathbf{x}_0 with given \mathbf{b} and \mathbf{A} . Here $m = 700$, $p = 0.1$, $\sigma_{\text{outliers}} = 10$. Figure 11 gives examples of image recovery for different MNIST images. From Figure 11, we can see that our algorithms outperform the PSGD algorithm. Table 3 presents that our algorithms perform better than the PSGD algorithm, both in terms of SNR and CPU time.

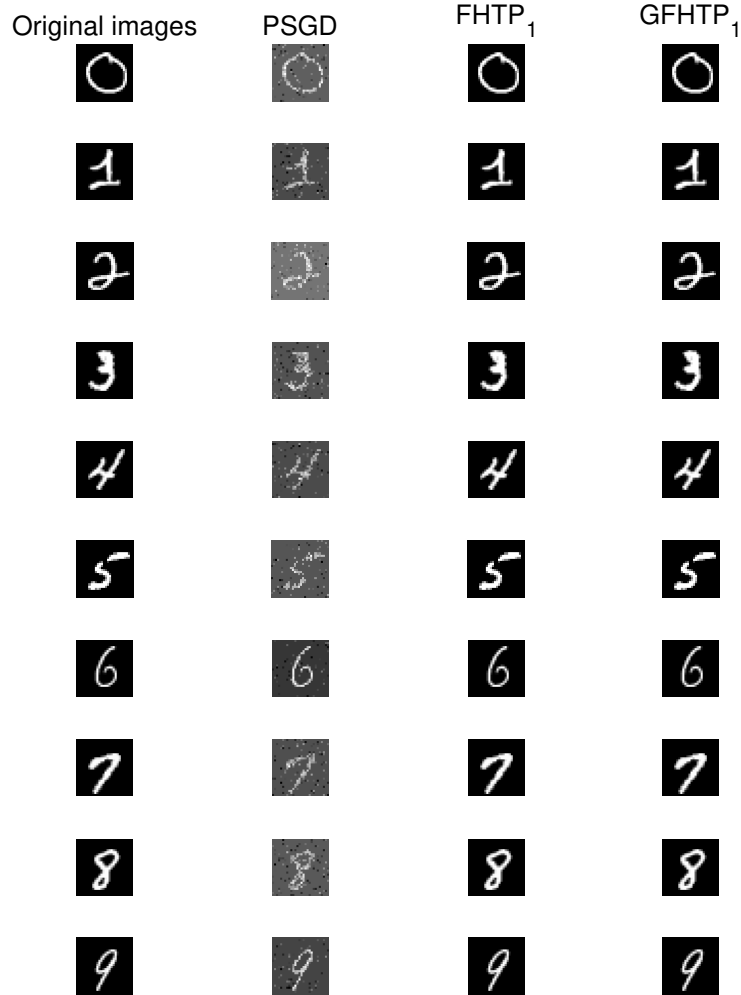


Figure 11: Examples of image recovery for different MNIST dataset images.

5 Conclusions

This study investigated the recovery of sparse signals using the graded fast hard thresholding pursuit (GFHTP₁) algorithm tailored for the least absolute deviations (LAD) model which has

Table 3: The SNR and average CPU time (s) by different algorithms for MNIST dataset images.

Original Images	PSGD	FHTP ₁	GFHTP ₁
Number 0 ($s = 138$)	3.9810,1.3670	88.7157,0.6711	85.4613,9.0405
Number 1 ($s = 139$)	4.3541,1.4701	89.8683,0.7665	90.2763 ,9.4709
Number 2 ($s = 150$)	3.4944,1.3526	97.4279,0.8991	96.2120,10.5938
Number 3 ($s = 155$)	3.1696,1.3157	102.8420,1.0409	90.5717,9.8892
Number 4 ($s = 130$)	3.5962,1.3465	111.0775,0.9729	110.1130,8.3666
Number 5 ($s = 111$)	2.8171,1.2974	93.1071,0.5612	93.4327 ,7.1790
Number 6 ($s = 107$)	8.6223,1.3339	87.3756,0.5871	86.6374,7.0019
Number 7 ($s = 144$)	2.9630,1.3464	105.1291,0.9642	84.1520,9.2865
Number 8 ($s = 158$)	3.2335,1.3159	89.6628,1.2815	96.4844 ,10.3156
Number 9 ($s = 108$)	5.4890,1.3764	102.5641,0.5188	103.1612 ,7.0324

the observations with outliers. We rigorously analyzed the convergence behavior of the proposed algorithm. Through numerical simulations, we observed that our method demonstrates superior performance relative to other algorithms, particularly when dealing with high outlier rates and unknown sparsity levels. Additionally, the proposed algorithm exhibited reduced computational complexity, which is particularly advantageous for large-scale experiments.

Acknowledgements

We would like to express our gratitude to Dr. Li-Ping Yin for her assistance in proving Theorem 2.5. This paper is supported by the National Natural Science Foundation of China (Nos. 12471353, 12201268), Fundamental Research Funds for the Central Universities (No. lzujbky-2024-it51).

Appendices

A Proof for General Sparse Signals

A.1 Preliminaries

In this subsection, we establish the foundational concepts and lemmas, including the restricted isometry property, the concentration property of sample quantile, and some necessary inequalities.

A.1.1 Restricted 1-Isometry Property (RIP₁)

We introduce a matrix that fulfills the RIP₁.

Lemma A.1. ([10, Lemma 3.2]) Suppose that $m \geq c_1 s \log(n/s)$ for some constant c_1 . Let $\mathbf{A} \in \mathbb{R}^{m \times n}$ ($m \ll n$) be a matrix with entries that are i.i.d. Gaussian random variables, i.e., $a_{ij} \sim \mathcal{N}(0, \frac{1}{m^2})$. Then, \mathbf{A} satisfies the RIP₁ of order s with a high probability exceeding $1 - 2 \exp(-\frac{m\delta_s^2}{16})$.

We also present a lemma that is instrumental in proving the main result in the subsequent section.

Lemma A.2. The matrix \mathbf{A} is assumed to satisfy the RIP₁, as defined in Lemma A.1. Let $W \subseteq [m]$ with $q = \frac{|W|}{m}$. Then, the submatrix $\mathbf{A}_W \in \mathbb{R}^{|W| \times n}$ of \mathbf{A} also satisfies the RIP₁, i.e., we have

$$(1 - \delta_s) \|\mathbf{x}\|_2 \leq \frac{1}{q} \sqrt{\frac{\pi}{2}} \|\mathbf{A}_W \mathbf{x}\|_1 \leq (1 + \delta_s) \|\mathbf{x}\|_2 \quad (\text{A.1})$$

for any s -sparse vector \mathbf{x} with high probability.

Proof. Since $a_{ij} \sim \mathcal{N}(0, \frac{1}{m^2})$, scaling by $\frac{1}{q}$ yields $\frac{1}{q}a_{ij} \sim \mathcal{N}(0, \frac{1}{(qm)^2})$. Noting that $qm = |W|$, this simplifies to $\frac{1}{q}a_{ij} \sim \mathcal{N}(0, \frac{1}{|W|^2})$. Consequently, the matrix \mathbf{A}_W satisfies the RIP₁. \square

A.1.2 Concentration Property of Sample Quantile

We proceed with the definition of the quantile of a population distribution and its sample counterpart.

Definition A.3. (*Generalized quantile function*). Let $0 < \omega < 1$. The generalized quantile function is defined as

$$F^{-1}(\omega) = \inf\{x \in \mathbb{R} : F(x) \geq \omega\}, \quad (\text{A.2})$$

where $F(\cdot)$ is a cumulative distribution function. For simplicity, we denote $\theta_\omega(F) = F^{-1}(\omega)$ as the ω -quantile of F . For a sample sequence $\{y_i\}_{i=1}^m$, the sample ω -quantile $\theta_\omega(\{y_i\}_{i=1}^m)$ refers to $\theta_\omega(\hat{F})$, with \hat{F} being the empirical distribution of the samples $\{y_i\}_{i=1}^m$.

We establish that as long as the sample size is sufficiently large, the sample quantile concentrates around the population quantile.

Lemma A.4. ([35, Lemma 1]) Suppose $F(\cdot)$ is cumulative distribution function with a continuous probability density function $f(\cdot)$. If the samples $\{y_i\}_{i=1}^m$ are i.i.d. drawn from f , and $0 < \omega < 1$, then the inequality

$$|\theta_\omega(\{y_i\}_{i=1}^m) - \theta_\omega(F)| < \epsilon$$

holds with a probability of at least $1 - 2\exp(-2m\epsilon^2 l^2)$, provided that $l < f(\theta) < L$ for all θ in the set $\{\theta : |\theta - \theta_\omega| \leq \epsilon\}$.

We also recall a result related to outliers.

Lemma A.5. ([35, Lemma 3], [22, Lemma A.3]) Consider clean samples $\{\tilde{y}_i\}_{i=1}^m$. If a fraction p of these samples are corrupted by outliers, the resulting contaminated samples $\{y_i\}_{i=1}^m$ contain pm corrupted samples and $(1-p)m$ clean samples. For a quantile τ such that $p < \tau < 1-p$, we have

$$\theta_{\tau-p}(\{\tilde{y}_i\}_{i=1}^m) \leq \theta_\tau(\{y_i\}_{i=1}^m) \leq \theta_{\tau+p}(\{\tilde{y}_i\}_{i=1}^m).$$

A.1.3 Some Necessary Inequalities

Lemma A.6. ([9, Lemma 7.3]) Suppose that $\mathbf{z} \in \mathbb{R}^n$ is generalized with i.i.d. Gaussian entries and $z_i \sim \mathcal{N}(0, \sigma^2)$, we have

$$\mathbb{P}\left(\|\mathbf{z}\|_2 \geq \sigma\sqrt{n + 2\sqrt{n \log n}}\right) \leq \frac{1}{n}.$$

Lemma A.7. ([8]) Let $\mathcal{D}_s = \{\mathbf{z} \in \mathbb{R}^n : \|\mathbf{z}\|_0 \leq s, \|\mathbf{z}\|_2 = 1\}$. Then there exists an ι -net $\bar{\mathcal{D}}_s \subset \mathcal{D}_s$ with respect to the ℓ_2 -norm obeying

$$|\bar{\mathcal{D}}_s| \leq \left(\frac{3n}{\iota}\right)^s.$$

A.2 Proofs of Propositions 3.1 and 3.2

Firstly, we give the proof of Proposition 3.1 in details.

Proof of Proposition 3.1. (i) First, we fix an arbitrary $(s+k)$ -sparse signal $\tilde{\mathbf{x}} \in \mathbb{R}^n$ satisfying $\|\tilde{\mathbf{x}}\|_2 = 1$, and subsequently generalize to all $(s+k)$ -sparse signals through a covering technique. It is noteworthy that the terms $m|\langle \mathbf{a}_i, \tilde{\mathbf{x}} \rangle|$, $i = 1, \dots, m$, are i.i.d. replicates of $m|\mathbf{A}\tilde{\mathbf{x}}|$. Here, the matrix \mathbf{A} is constructed with i.i.d. Gaussian entries $\mathcal{N}(0, \frac{1}{m^2})$. Given that $\|\tilde{\mathbf{x}}\|_2 = 1$, the vector

$m\mathbf{A}\tilde{\mathbf{x}}$ follows a standard normal distribution $\mathcal{N}(\mathbf{0}, \mathbf{I}_m)$, and thus $m|\mathbf{A}\tilde{\mathbf{x}}|$ follows a folded normal distribution. As established in Lemma A.4, the τ -quantile $m\theta_\tau(|\mathbf{A}\tilde{\mathbf{x}}|)$ satisfies the inequality:

$$\Phi^{-1}\left(\frac{1+\tau}{2}\right) - \epsilon \leq m\theta_\tau(|\mathbf{A}\tilde{\mathbf{x}}|) \leq \Phi^{-1}\left(\frac{1+\tau}{2}\right) + \epsilon \quad (\text{A.3})$$

with a probability of at least $1 - 2\exp(-dme^2)$ for a small positive value ϵ , where d is a constant approximately equal to $2 \times (2\phi(\frac{1+\tau}{2}))^2$, and ϕ represents the probability density function of the standard Gaussian distribution.

Next, we generalize the above result to all $(s+k)$ -sparse signals \mathbf{x} with $\|\mathbf{x}\|_2 = 1$ by leveraging a covering argument. Let \mathcal{N}_ι stand for an ι -net that covers the set of all $(s+k)$ -sparse signals under the ℓ_2 -norm. According to Lemma A.7, the cardinality of \mathcal{N}_ι satisfies $|\mathcal{N}_\iota| \leq (\frac{3n}{\iota})^{s+k}$. Employing the union bound, we can derive that

$$\Phi^{-1}\left(\frac{1+\tau}{2}\right) - \epsilon \leq m\theta_\tau(|\mathbf{A}\tilde{\mathbf{x}}|) \leq \Phi^{-1}\left(\frac{1+\tau}{2}\right) + \epsilon, \quad \forall \tilde{\mathbf{x}} \in \mathcal{N}_\iota \quad (\text{A.4})$$

holds with probability at least $1 - 2(\frac{3n}{\iota})^{s+k} \exp(-dme^2)$. We set $\iota = \frac{\epsilon}{\sqrt{n+2\sqrt{n \log n}}}$. Under this event and Lemma A.6, for any $(s+k)$ -sparse signal \mathbf{x} with $\|\mathbf{x}\|_2 = 1$, there exists a signal $\tilde{\mathbf{x}} \in \mathcal{N}_\iota$ such that $\|\mathbf{x} - \tilde{\mathbf{x}}\|_2 \leq \iota$. Furthermore, by Lemma 2 of [35], the following inequality holds

$$\begin{aligned} |m\theta_\tau(|\mathbf{A}\tilde{\mathbf{x}}|) - m\theta_\tau(|\mathbf{A}\mathbf{x}|)| &\leq \max_i m |\langle \mathbf{a}_i, \tilde{\mathbf{x}} \rangle| - |\langle \mathbf{a}_i, \mathbf{x} \rangle| \\ &\leq \max_i m |\langle \mathbf{a}_i, \tilde{\mathbf{x}} \rangle - \langle \mathbf{a}_i, \mathbf{x} \rangle| \\ &\leq \max_i m \|\mathbf{x} - \tilde{\mathbf{x}}\|_2 \|\mathbf{a}_i\|_2 \\ &\leq \iota \max_i \|m\mathbf{a}_i\|_2 \leq \epsilon \end{aligned} \quad (\text{A.5})$$

with a probability of at least $1 - 2(\frac{3n}{\iota})^{s+k} \exp(-dme^2) - \frac{1}{n}$.

The remaining part of the proof is to argue that (A.5) holds with probability at least $1 - d_1 \exp(-d_2 m \epsilon^2) - \frac{1}{n}$, where d_1 and d_2 are some constants. This is valid provided that $m \geq d_0(\epsilon^{-2} \log(\epsilon^{-1}))(s+k) \log n$ for a sufficiently large constant d_0 . To verify this, we first analyze the term $(\frac{3n}{\iota})^{s+k}$:

$$\begin{aligned} \left(\frac{3n}{\iota}\right)^{s+k} &= \exp\left((s+k) \log\left(\frac{3n}{\iota}\right)\right) \\ &= \exp\left((s+k) \left(\log 3 + \log n + \frac{1}{2} \log(n + 2\sqrt{n \log n}) + \log(\epsilon^{-1})\right)\right) \\ &\leq \exp\left((s+k) \left(\frac{3}{2} \log 3 + \frac{3}{2} \log n + \log(\epsilon^{-1})\right)\right) \\ &\leq (3(s+k) \log n + (s+k) \log(\epsilon^{-1})), \end{aligned}$$

where the first inequality is derived from the fact that $\log n < n$. It is easy to conform that $3(s+k) \log n < d_3 m \epsilon^2$ and $(s+k) \log(\epsilon^{-1}) \leq d_4 m \epsilon^2$. Based on the specific formulation of m , as long as the constant d_0 is chosen to be sufficiently large, we can obtain

$$2 \left(\frac{3n}{\iota}\right)^{s+k} \exp(-dme^2) < d_1 \exp(-d_2 m \epsilon^2).$$

Here, $d_3 + d_4 < d - d_2$.

(ii) We first address the upper bound for $\|(\mathbf{b} - \mathbf{A}\mathbf{x}) \odot (\mathbb{I}_{\{|\mathbf{b}_i - (\mathbf{A}\mathbf{x})_i| \leq \theta_\tau(|\mathbf{b} - \mathbf{A}\mathbf{x}|)\}})_{i=1}^m\|_1$:

$$\|(\mathbf{b} - \mathbf{A}\mathbf{x}) \odot (\mathbb{I}_{\{|\mathbf{b}_i - (\mathbf{A}\mathbf{x})_i| \leq \theta_\tau(|\mathbf{b} - \mathbf{A}\mathbf{x}|)\}})_{i=1}^m\|_1 \leq \tau m \theta_\tau(|\mathbf{b} - \mathbf{A}\mathbf{x}|)$$

$$\begin{aligned}
&\leq \tau m \theta_{\tau+p}(|\mathbf{A}(\mathbf{x}_0 - \mathbf{x})|) \\
&\leq \tau \left(\Phi^{-1} \left(\frac{1+\tau+p}{2} \right) + \epsilon \right) \|\mathbf{x} - \mathbf{x}_0\|_2,
\end{aligned}$$

where the second inequality is derived from Lemma A.5, and the last inequality holds with high probability for a small ϵ from Item (i) above. Next, we establish the lower bound for $\|(\mathbf{b} - \mathbf{Ax}) \odot (\mathbb{I}_{\{|b_i - (\mathbf{Ax})_i| \leq \theta_\tau(|\mathbf{b} - \mathbf{Ax}|)\}})_{i=1}^m\|_1$:

$$\begin{aligned}
\|(\mathbf{b} - \mathbf{Ax}) \odot (\mathbb{I}_{\{|b_i - (\mathbf{Ax})_i| \leq \theta_\tau(|\mathbf{b} - \mathbf{Ax}|)\}})_{i=1}^m\|_1 &= \|(\mathbf{A}_{T_1}(\mathbf{x}_0 - \mathbf{x}) + \boldsymbol{\eta}_{T_1})\|_1 + \|\mathbf{A}_{T_2}(\mathbf{x}_0 - \mathbf{x})\|_1 \\
&\geq \|\mathbf{A}_{T_2}(\mathbf{x}_0 - \mathbf{x})\|_1 \\
&\geq \left(\tau - \frac{|T_1|}{m} \right) \sqrt{\frac{2}{\pi}} (1 - \delta_{s+l}) \|\mathbf{x} - \mathbf{x}_0\|_2,
\end{aligned}$$

where $T_1 = T \cap \Gamma$, $T_2 = \Gamma \setminus T_1$ with $|T_1 \cup T_2| = \tau m$ and $|T_1|$ is a small number. Thus the proof is finished. \square

Next, we turn our attention to Proposition 3.2.

Proof of Proposition 3.2. For $\|[\mathbf{x}_0 - \mathbf{u}^{k,l} - t_{k,l} \mathbf{A}^\top \text{sign}(\mathbf{b} - \mathbf{A}\mathbf{u}^{k,l})]_{\Lambda^k}\|_2^2$, it can be equivalently expressed as:

$$\begin{aligned}
&\|[\mathbf{x}_0 - \mathbf{u}^{k,l} - t_{k,l} \mathbf{A}^\top \text{sign}(\mathbf{b} - \mathbf{A}\mathbf{u}^{k,l})]_{\Lambda^k}\|_2^2 \\
&= \|\mathbf{x}_0 - \mathbf{u}^{k,l}\|_2^2 + t_{k,l}^2 \|\mathbf{A}^\top \text{sign}(\mathbf{b} - \mathbf{A}\mathbf{u}^{k,l})]_{\Lambda^k}\|_2^2 \\
&\quad - 2t_{k,l} \langle \mathbf{x}_0 - \mathbf{u}^{k,l}, [\mathbf{A}^\top \text{sign}(\mathbf{b} - \mathbf{A}\mathbf{u}^{k,l})]_{\Lambda^k} \rangle \\
&=: \|\mathbf{x}_0 - \mathbf{u}^{k,l}\|_2^2 + t_{k,l}^2 F_1 - 2t_{k,l} F_2.
\end{aligned} \tag{A.6}$$

Next, we estimate the upper bound of F_1 and the lower bound of F_2 . Using the RIP₁, we can bound F_1 as follows:

$$\begin{aligned}
F_1 &= \langle \mathbf{A}^\top \text{sign}(\mathbf{b} - \mathbf{A}\mathbf{u}^{k,l}), [\mathbf{A}^\top \text{sign}(\mathbf{b} - \mathbf{A}\mathbf{u}^{k,l})]_{\Lambda^k} \rangle \\
&= \langle \text{sign}(\mathbf{b} - \mathbf{A}\mathbf{u}^{k,l}), \mathbf{A}[\mathbf{A}^\top \text{sign}(\mathbf{b} - \mathbf{A}\mathbf{u}^{k,l})]_{\Lambda^k} \rangle \\
&\leq \|\mathbf{A}[\mathbf{A}^\top \text{sign}(\mathbf{b} - \mathbf{A}\mathbf{u}^{k,l})]_{\Lambda^k}\|_1 \\
&\leq \sqrt{\frac{2}{\pi}} (1 + \delta_{2k+s-1}) \|\mathbf{A}^\top \text{sign}(\mathbf{b} - \mathbf{A}\mathbf{u}^{k,l})]_{\Lambda^k}\|_2,
\end{aligned}$$

thus we can get the estimation of F_1 as follows

$$F_1 \leq \frac{2}{\pi} (1 + \delta_{2k+s-1})^2. \tag{A.7}$$

For the lower bound of F_2 , we have

$$\begin{aligned}
F_2 &= \langle \mathbf{x}_0 - \mathbf{u}^{k,l}, \mathbf{A}^\top \text{sign}(\mathbf{b} - \mathbf{A}\mathbf{u}^{k,l}) \rangle = \langle \mathbf{A}(\mathbf{x}_0 - \mathbf{u}^{k,l}), \text{sign}(\mathbf{b} - \mathbf{A}\mathbf{u}^{k,l}) \rangle \\
&= \langle \mathbf{A}_T(\mathbf{x}_0 - \mathbf{u}^{k,l}), \text{sign}(\mathbf{A}_T(\mathbf{x}_0 - \mathbf{u}^{k,l}) + \boldsymbol{\eta}_T) \rangle \\
&\quad + \langle \mathbf{A}_{T^c}(\mathbf{x}_0 - \mathbf{u}^{k,l}), \text{sign}(\mathbf{A}_{T^c}(\mathbf{x}_0 - \mathbf{u}^{k,l})) \rangle \\
&= \langle \mathbf{A}_T(\mathbf{x}_0 - \mathbf{u}^{k,l}) + \boldsymbol{\eta}_T, \text{sign}(\mathbf{A}_T(\mathbf{x}_0 - \mathbf{u}^{k,l}) + \boldsymbol{\eta}_T) \rangle \\
&\quad - \langle \boldsymbol{\eta}_T, \text{sign}(\mathbf{A}_T(\mathbf{x}_0 - \mathbf{u}^{k,l}) + \boldsymbol{\eta}_T) \rangle + \|\mathbf{A}_{T^c}(\mathbf{x}_0 - \mathbf{u}^{k,l})\|_1 \\
&\geq \|\mathbf{A}_T(\mathbf{x}_0 - \mathbf{u}^{k,l}) + \boldsymbol{\eta}_T\|_1 - \|\boldsymbol{\eta}_T\|_1 + \|\mathbf{A}_{T^c}(\mathbf{x}_0 - \mathbf{u}^{k,l})\|_1 \\
&\geq -\|\mathbf{A}_T(\mathbf{x}_0 - \mathbf{u}^{k,l})\|_1 + \|\mathbf{A}_{T^c}(\mathbf{x}_0 - \mathbf{u}^{k,l})\|_1
\end{aligned}$$

$$\begin{aligned}
&= -\|\mathbf{A}(\mathbf{x}_0 - \mathbf{u}^{k,l})\|_1 + 2\|\mathbf{A}_{T^c}(\mathbf{x}_0 - \mathbf{u}^{k,l})\|_1 \\
&\geq \sqrt{\frac{2}{\pi}}[(2-2p)(1-\delta_{2k+s-1}) - (1+\delta_{2k+s-1})]\|\mathbf{x}_0 - \mathbf{u}^{k,l}\|_2 \\
&=: \sqrt{\frac{2}{\pi}}c_k\|\mathbf{x}_0 - \mathbf{u}^{k,l}\|_2,
\end{aligned} \tag{A.8}$$

where the last inequality comes from RIP₁ and Lemma A.2, and $c_k = (2-2p)(1-\delta_{2k+s-1}) - (1+\delta_{2k+s-1})$. Combining the bounds for F_1 and F_2 with (A.6), we arrive at

$$\begin{aligned}
&\|[\mathbf{x}_0 - \mathbf{u}^{k,l} - t_{k,l}\mathbf{A}^\top \text{sign}(\mathbf{b} - \mathbf{A}\mathbf{u}^{k,l})]_{\Lambda^k}\|_2^2 \\
&\leq \|\mathbf{x}_0 - \mathbf{u}^{k,l}\|_2^2 + t_{k,l}^2 \frac{2}{\pi} (1 + \delta_{2k+s-1})^2 - 2t_{k,l} \sqrt{\frac{2}{\pi}} c_k \|\mathbf{x}_0 - \mathbf{u}^{k,l}\|_2 \\
&= \|\mathbf{x}_0 - \mathbf{u}^{k,l}\|_2^2 + \mu_{k,l}^2 (1 + \delta_{2k+s-1})^2 \|(\mathbf{b} - \mathbf{A}\mathbf{u}^{k,l}) \odot (\mathbb{I}_{\{|b_i - (\mathbf{A}\mathbf{u}^{k,l})_i| \leq \theta_\tau(|\mathbf{b} - \mathbf{A}\mathbf{u}^{k,l}|)\}})_{i=1}^m\|_1^2 \\
&\quad - 2\mu_{k,l} c_k \|(\mathbf{b} - \mathbf{A}\mathbf{u}^{k,l}) \odot (\mathbb{I}_{\{|b_i - (\mathbf{A}\mathbf{u}^{k,l})_i| \leq \theta_\tau(|\mathbf{b} - \mathbf{A}\mathbf{u}^{k,l}|)\}})_{i=1}^m\|_1 \|\mathbf{x}_0 - \mathbf{u}^{k,l}\|_2 \\
&\leq \left(1 + \tau^2(\Phi^{-1} + \epsilon)^2 (1 + \delta_{2k+s-1})^2 \mu_{k,l}^2 - 2c_k \sqrt{\frac{2}{\pi}} \left(\tau - \frac{|T_1^{k,l}|}{m}\right) (1 - \delta_{2k+s-1}) \mu_{k,l}\right) \|\mathbf{x}_0 - \mathbf{u}^{k,l}\|_2^2 \\
&=: \rho_{k,l} \|\mathbf{x}_0 - \mathbf{u}^{k,l}\|_2^2,
\end{aligned}$$

where the last inequality is from Proposition 3.1. Thus we finish the proof. \square

A.3 Proof of Theorem 2.2

In this subsection, we show the proof of Theorem 2.2 in details.

Proof of Theorem 2.2. Firstly, we proceed with the analysis by defining the supports of the vectors involved in the iterative process. Let S, S^{k-1} and $S^k (k \geq s)$ denote the supports of $\mathbf{x}_0, \mathbf{x}^{k-1}$ (or $\mathbf{u}^{k,0}$), and $\mathbf{u}^{k,l}$ for $1 \leq l \leq L+1$, respectively, and let $\Lambda^k := S \cup S^{k-1} \cup S^k$.

We now focus on bounding the term $\|\mathbf{x}_0 - \mathbf{u}^{k,l+1}\|_2^2$. It follows from the update scheme (2.5) that

$$\begin{aligned}
\|\mathbf{x}_0 - \mathbf{u}^{k,l+1}\|_2^2 &= \|(\mathbf{x}_0 - \mathbf{u}^{k,l+1})_{S^k}\|_2^2 + \|(\mathbf{x}_0 - \mathbf{u}^{k,l+1})_{(S^k)^c}\|_2^2 \\
&= \|[\mathbf{x}_0 - \mathbf{u}^{k,l} - t_{k,l}\mathbf{A}^\top \text{sign}(\mathbf{b} - \mathbf{A}\mathbf{u}^{k,l})]_{S^k}\|_2^2 + \|(\mathbf{x}_0)_{S \setminus S^k}\|_2^2 \\
&\leq \|[\mathbf{x}_0 - \mathbf{u}^{k,l} - t_{k,l}\mathbf{A}^\top \text{sign}(\mathbf{b} - \mathbf{A}\mathbf{u}^{k,l})]_{\Lambda^k}\|_2^2 + \|(\mathbf{x}_0)_{S \setminus S^k}\|_2^2 \\
&=: E_1 + E_2.
\end{aligned} \tag{A.9}$$

To achieve this, we consider the upper bounds of the terms E_1 and E_2 .

Note that it follows from Proposition 3.2 that

$$E_1 \leq \rho_{k,l} \|\mathbf{x}_0 - \mathbf{u}^{k,l}\|_2^2. \tag{A.10}$$

Therefore, it remains to estimate E_2 . We claim that E_2 satisfies

$$E_2 \leq 2\rho_{k,0} \|\mathbf{x}_0 - \mathbf{x}^{k-1}\|_2^2. \tag{A.11}$$

By substituting the two bounds above into (A.9), one has

$$\|\mathbf{x}_0 - \mathbf{u}^{k,l+1}\|_2^2 \leq \rho_{k,l} \|\mathbf{x}_0 - \mathbf{u}^{k,l}\|_2^2 + 2\rho_{k,0} \|\mathbf{x}_0 - \mathbf{x}^{k-1}\|_2^2. \tag{A.12}$$

Moreover, by conducting immediate induction on l with $\mathbf{u}^{k,0} =: \mathbf{x}^{k-1}$ and $\mathbf{u}^{k,L+1} =: \mathbf{x}^k$, we have

$$\begin{aligned}
\|\mathbf{x}_0 - \mathbf{x}^k\|_2^2 &= \|\mathbf{x}_0 - \mathbf{u}^{k,L+1}\|_2^2 \\
&\leq \rho_{k,L} \|\mathbf{x}_0 - \mathbf{u}^{k,L}\|_2^2 + 2\rho_{k,0} \|\mathbf{x}_0 - \mathbf{x}^{k-1}\|_2^2 \\
&\leq \rho_{k,L} (\rho_{k,L-1} \|\mathbf{x}_0 - \mathbf{u}^{k,L-1}\|_2^2 + 2\rho_{k,0} \|\mathbf{x}_0 - \mathbf{x}^{k-1}\|_2^2) + 2\rho_{k,0} \|\mathbf{x}_0 - \mathbf{x}^{k-1}\|_2^2 \\
&= \left(\prod_{l=L-1}^L \rho_{k,l} \right) \|\mathbf{x}_0 - \mathbf{u}^{k,L-1}\|_2^2 + 2\rho_{k,0} (1 + \rho_{k,L}) \|\mathbf{x}_0 - \mathbf{x}^{k-1}\|_2^2 \\
&\leq \dots \\
&\leq \left(\prod_{l=0}^L \rho_{k,l} \right) \|\mathbf{x}_0 - \mathbf{u}^{k,0}\|_2^2 + 2\rho_{k,0} \left(1 + \sum_{i=1}^L \prod_{l=i}^L \rho_{k,l} \right) \|\mathbf{x}_0 - \mathbf{x}^{k-1}\|_2^2. \tag{A.13}
\end{aligned}$$

In summary, due to $\rho_k = \max_l \rho_{k,l}$, we obtain

$$\begin{aligned}
\|\mathbf{x}_0 - \mathbf{x}^k\|_2^2 &\leq \left(\prod_{l=0}^L \rho_k \right) \|\mathbf{x}_0 - \mathbf{x}^{k-1}\|_2^2 + 2\rho_k \left(1 + \sum_{i=1}^L \prod_{l=i}^L \rho_k \right) \|\mathbf{x}_0 - \mathbf{x}^{k-1}\|_2^2 \\
&= (\rho_k^{L+1} + 2\rho_k (\rho_k^L + \rho_k^{L-1} + \dots + \rho_k + 1)) \|\mathbf{x}_0 - \mathbf{x}^{k-1}\|_2^2 \\
&= \left(\rho_k^{L+1} + 2\rho_k \frac{1 - \rho_k^{L+1}}{1 - \rho_k} \right) \|\mathbf{x}_0 - \mathbf{x}^{k-1}\|_2^2 \\
&= \left(\frac{\rho_k^{L+1}(1 - 3\rho_k) + 2\rho_k}{1 - \rho_k} \right) \|\mathbf{x}_0 - \mathbf{x}^{k-1}\|_2^2.
\end{aligned}$$

Here, the condition 2.7 implies that $\frac{\rho_k^{L+1}(1 - 3\rho_k) + 2\rho_k}{1 - \rho_k} < 1$.

To conclude, proving the inequality (A.11) is sufficient to establish the conclusion. Since S^k is the index set of k largest absolute entries of $\mathbf{x}^{k-1} + t_{k,0} \mathbf{A}^\top \text{sign}(\mathbf{b} - \mathbf{A}\mathbf{x}^{k-1})$, then we notice that

$$\|(\mathbf{x}^{k-1} + t_{k,0} \mathbf{A}^\top \text{sign}(\mathbf{b} - \mathbf{A}\mathbf{x}^{k-1}))_{S^k}\|_2 \geq \|(\mathbf{x}^{k-1} + t_{k,0} \mathbf{A}^\top \text{sign}(\mathbf{b} - \mathbf{A}\mathbf{x}^{k-1}))_S\|_2.$$

By eliminating the contribution on $S \cap S^k$, we obtain

$$\|(\mathbf{x}^{k-1} + t_{k,0} \mathbf{A}^\top \text{sign}(\mathbf{b} - \mathbf{A}\mathbf{x}^{k-1}))_{S^k \setminus S}\|_2 \geq \|(\mathbf{x}^{k-1} + t_{k,0} \mathbf{A}^\top \text{sign}(\mathbf{b} - \mathbf{A}\mathbf{x}^{k-1}))_{S \setminus S^k}\|_2. \tag{A.14}$$

The left-hand side satisfies

$$\|(\mathbf{x}^{k-1} + t_{k,0} \mathbf{A}^\top \text{sign}(\mathbf{b} - \mathbf{A}\mathbf{x}^{k-1}))_{S^k \setminus S}\|_2 = \|(\mathbf{x}^{k-1} - \mathbf{x}_0 + t_{k,0} \mathbf{A}^\top \text{sign}(\mathbf{b} - \mathbf{A}\mathbf{x}^{k-1}))_{S^k \setminus S}\|_2,$$

while the right-hand side satisfies

$$\|(\mathbf{x}^{k-1} + t_{k,0} \mathbf{A}^\top \text{sign}(\mathbf{b} - \mathbf{A}\mathbf{x}^{k-1}))_{S \setminus S^k}\|_2 \geq \|(\mathbf{x}_0)_{S \setminus S^k}\|_2 - \|(\mathbf{x}^{k-1} - \mathbf{x}_0 + t_{k,0} \mathbf{A}^\top \text{sign}(\mathbf{b} - \mathbf{A}\mathbf{x}^{k-1}))_{S \setminus S^k}\|_2.$$

Consequently, substituting the two estimations above into the inequality (A.14), we get

$$\begin{aligned}
E_2^{\frac{1}{2}} &= \|(\mathbf{x}_0)_{S \setminus S^k}\|_2 \leq \|(\mathbf{x}^{k-1} - \mathbf{x}_0 + t_{k,0} \mathbf{A}^\top \text{sign}(\mathbf{b} - \mathbf{A}\mathbf{x}^{k-1}))_{S \setminus S^k}\|_2 \\
&\quad + \|(\mathbf{x}^{k-1} - \mathbf{x}_0 + t_{k,0} \mathbf{A}^\top \text{sign}(\mathbf{b} - \mathbf{A}\mathbf{x}^{k-1}))_{S^k \setminus S}\|_2 \\
&\leq \sqrt{2} \|(\mathbf{x}^{k-1} - \mathbf{x}_0 + t_{k,0} \mathbf{A}^\top \text{sign}(\mathbf{b} - \mathbf{A}\mathbf{x}^{k-1}))_{S \setminus S^k}\|_2 \\
&\leq \sqrt{2} \|(\mathbf{x}^{k-1} - \mathbf{x}_0 + t_{k,0} \mathbf{A}^\top \text{sign}(\mathbf{b} - \mathbf{A}\mathbf{x}^{k-1}))_{\Lambda_k}\|_2 \\
&\leq \sqrt{2\rho_{k,0}} \|\mathbf{x}_0 - \mathbf{x}^{k-1}\|_2,
\end{aligned}$$

where the last inequality is from $E_1 = \|[\mathbf{x}_0 - \mathbf{u}^{k,l} - t_{k,l} \mathbf{A}^\top \text{sign}(\mathbf{b} - \mathbf{A}\mathbf{u}^{k,l})]_{\Lambda^k}\|_2^2$ and Proposition 3.2 with $l = 0$. Thus, we get the estimation for E_2 . Thus we finish the conclusion. \square

B Proof for Structured Sparse Signals

B.1 Proof of Proposition 3.3

Proof. Firstly, we claim that

$$\begin{aligned} \|\mathbf{x}^{k-1} - \mathbf{x}_0\|_2^2 &\leq 2(\beta_k + \tau^2(\Phi^{-1} + \epsilon)^2(1 + \delta_s)^2\mu_{k,0}^2)\|\mathbf{x}_0 - \mathbf{x}^{k-1}\|_2^2 + \|(\mathbf{x}_0)_{(S^{k-1})^c}\|_2^2 \\ &=: 2\beta'_k\|\mathbf{x}^{k-1} - \mathbf{x}_0\|_2^2 + \|(\mathbf{x}_0)_{(S^{k-1})^c}\|_2^2, \end{aligned} \quad (\text{B.1})$$

where $\beta_k = 1 + \tau^2(\Phi^{-1} + \epsilon)^2(1 + \delta_s)^2\mu_{k,0}^2 - 2c\sqrt{\frac{2}{\pi}}\left(\tau - \frac{|T_1^{k,0}|}{m}\right)(1 - \delta_s)\mu_{k,0}$. And the upper bound of ξ_k satisfies

$$\begin{aligned} \xi_k &= t_{k,0} \max_{\ell \in S^c} |\mathbf{A}^\top \text{sign}(\mathbf{b} - \mathbf{A}\mathbf{x}^{k-1}))_\ell| \\ &\leq \mu_{k,0} \sqrt{\frac{\pi}{2}}\tau(\Phi^{-1} + \epsilon)\|\mathbf{x}^{k-1} - \mathbf{x}_0\|_2 \max_{\ell \in S^c} |\mathbf{A}^\top \text{sign}(\mathbf{b} - \mathbf{A}\mathbf{x}^{k-1}))_\ell|, \end{aligned} \quad (\text{B.2})$$

and the lower bound of ζ_k is

$$\zeta_k \geq \frac{1}{\sqrt{s-k+1}} \left(\frac{\sqrt{1-2\beta'_k}}{\lambda} - \sqrt{\beta_k} \right) \|\mathbf{x}^{k-1} - \mathbf{x}_0\|_2. \quad (\text{B.3})$$

By the combination of estimations (B.2) and (B.3), we have

$$\begin{aligned} &\mathbb{P}(\xi_k \geq \zeta_k) \\ &\leq \mathbb{P} \left(\mu_{k,0} \sqrt{\frac{\pi}{2}}\tau(\Phi^{-1} + \epsilon) \max_{\ell \in S^c} |\langle \mathbf{A}^\top \text{sign}(\mathbf{b} - \mathbf{A}\mathbf{x}^{k-1}) \rangle_\ell| \geq \frac{1}{\sqrt{s-k+1}} \left(\frac{\sqrt{1-2\beta'_k}}{\lambda} - \sqrt{\beta_k} \right) \right) \\ &= \mathbb{P} \left(\max_{\ell \in S^c} |\langle \tilde{\mathbf{a}}_\ell, \text{sign}(\mathbf{b} - \mathbf{A}\mathbf{x}^{k-1}) \rangle| \geq \frac{\sqrt{\frac{2}{\pi}}}{\sqrt{s-k+1}\mu_{k,0}\tau(\Phi^{-1} + \epsilon)} \left(\frac{\sqrt{1-2\beta'_k}}{\lambda} - \sqrt{\beta_k} \right) \right) \\ &\leq \mathbb{P} \left(\max_{\ell \in S^c} |\langle \tilde{\mathbf{a}}_\ell, \text{sign}(\mathbf{b} - \mathbf{A}\mathbf{x}^{k-1}) \rangle| \geq \frac{\sqrt{\frac{2}{\pi}}}{\sqrt{s}\mu_{k,0}\tau(\Phi^{-1} + \epsilon)} \left(\frac{\sqrt{1-2\beta'_k}}{\lambda} - \sqrt{\beta_k} \right) \right) \\ &=: \mathbb{P} \left(\max_{\ell \in S^c} |\langle \tilde{\mathbf{a}}_\ell, \text{sign}(\mathbf{b} - \mathbf{A}\mathbf{x}^{k-1}) \rangle| \geq \frac{\gamma_k}{\sqrt{s}} \right), \end{aligned}$$

where $\mathbf{A} = [\tilde{\mathbf{a}}_1, \dots, \tilde{\mathbf{a}}_n]$. Note that for the sum of these random variables $S_m = X_1 + \dots + X_m$ with independent and bounded random variables $X_j \in [a_j, b_j]$ for $j = 1, \dots, m$, the Hoeffding's inequality [16] states that for all $t > 0$, $\mathbb{P}(|S_m - \mathbb{E}(S_m)| \geq t) \leq 2\exp(-2t^2/\sum_{j=1}^m (b_j - a_j)^2)$. Thus, from $\mathbb{E}\langle \tilde{\mathbf{a}}_\ell, \text{sign}(\mathbf{b} - \mathbf{A}\mathbf{x}^{k-1}) \rangle = 0$, we can conclude that

$$\begin{aligned} \mathbb{P}(\xi_k \geq \zeta_k) &\leq \sum_{\ell \in S^c} \mathbb{P} \left(|\langle \tilde{\mathbf{a}}_\ell, \text{sign}(\mathbf{b} - \mathbf{A}\mathbf{x}^{k-1}) \rangle| \geq \frac{\gamma_k}{\sqrt{s}} \right) \\ &\leq 2(n-s) \exp \left(-\frac{\gamma_k^2}{2s(\max_\ell \|\tilde{\mathbf{a}}_\ell\|_2^2)} \right) \\ &\leq 2(n-s) \exp \left(-\frac{\gamma_k^2}{2s \left(\frac{1}{m} \sqrt{m + 2\sqrt{m \log m}} \right)^2} \right) \\ &\leq 2(n-s) \exp \left(-\frac{\gamma_k^2 m}{6s} \right), \end{aligned}$$

where the third inequality is derived from Lemma A.6.

To conclude, it is sufficient to prove the three estimations (B.1), (B.2) and (B.3).

(i) Proof of the Inequality (B.1). Using the triangle inequality and the RIP₁ condition, we obtain

$$\begin{aligned}
\|\mathbf{x}^{k-1} - \mathbf{x}_0\|_2^2 &= \|(\mathbf{x}^{k-1} - \mathbf{x}_0)_{S^{k-1}}\|_2^2 + \|(\mathbf{x}^{k-1} - \mathbf{x}_0)_{(S^{k-1})^c}\|_2^2 \\
&\leq 2\|(\mathbf{x}^{k-1} - \mathbf{x}_0 + t_{k,0}\mathbf{A}^\top \text{sign}(\mathbf{b} - \mathbf{A}\mathbf{x}^{k-1}))_{S^{k-1}}\|_2^2 \\
&\quad + 2t_{k,0}^2\|(\mathbf{A}^\top \text{sign}(\mathbf{b} - \mathbf{A}\mathbf{x}^{k-1}))_{S^{k-1}}\|_2^2 + \|(\mathbf{x}_0)_{(S^{k-1})^c}\|_2^2 \\
&\leq 2\|(\mathbf{x}^{k-1} - \mathbf{x}_0 + t_{k,0}\mathbf{A}^\top \text{sign}(\mathbf{b} - \mathbf{A}\mathbf{x}^{k-1}))_S\|_2^2 \\
&\quad + 2t_{k,0}^2\|(\mathbf{A}^\top \text{sign}(\mathbf{b} - \mathbf{A}\mathbf{x}^{k-1}))_S\|_2^2 + \|(\mathbf{x}_0)_{(S^{k-1})^c}\|_2^2,
\end{aligned} \tag{B.4}$$

where the second inequality comes from $S^{k-1} \subseteq S$. Notice that by the estimation (A.7) and Proposition 3.1, one has

$$\begin{aligned}
t_{k,0}^2\|(\mathbf{A}^\top \text{sign}(\mathbf{b} - \mathbf{A}\mathbf{x}^{k-1}))_S\|_2^2 &=: t_{k,0}^2 G_1 \\
&\leq \frac{2}{\pi}(1 + \delta_s)^2 \left(\mu_{k,0} \sqrt{\frac{\pi}{2}} \|(\mathbf{b} - \mathbf{A}\mathbf{x}^{k-1}) \odot (\mathbb{I}_{\{|b_i - (\mathbf{A}\mathbf{x}^{k-1})_i| \leq \theta_\tau(|\mathbf{b} - \mathbf{A}\mathbf{x}^{k-1}|)\}})_{i=1}^m \|_1 \right)^2 \\
&\leq \tau^2(\Phi^{-1} + \epsilon)^2(1 + \delta_s)^2 \mu_{k,0}^2 \|\mathbf{x}_0 - \mathbf{x}^{k-1}\|_2^2.
\end{aligned} \tag{B.5}$$

Given that $\zeta_{k-1} > \xi_{k-1}$ implies $S^{k-1} \subseteq S$, we can further get

$$\begin{aligned}
&\|(\mathbf{x}^{k-1} - \mathbf{x}_0 + t_{k,0}\mathbf{A}^\top \text{sign}(\mathbf{b} - \mathbf{A}\mathbf{x}^{k-1}))_S\|_2^2 \\
&= \|\mathbf{x}^{k-1} - \mathbf{x}_0\|_2^2 + t_{k,0}^2\|(\mathbf{A}^\top \text{sign}(\mathbf{b} - \mathbf{A}\mathbf{x}^{k-1}))_S\|_2^2 - 2t_{k,0}\langle \mathbf{x}_0 - \mathbf{x}^{k-1}, (\mathbf{A}^\top \text{sign}(\mathbf{b} - \mathbf{A}\mathbf{x}^{k-1}))_S \rangle \\
&=: \|\mathbf{x}^{k-1} - \mathbf{x}_0\|_2^2 + t_{k,0}^2 G_1 - 2t_{k,0} G_2.
\end{aligned} \tag{B.6}$$

Consequently, leveraging a proof strategy analogous to that employed in Proposition 3.2, we can straightly derive the following desired result

$$\begin{aligned}
&\|(\mathbf{x}^{k-1} - \mathbf{x}_0 + t_{k,0}\mathbf{A}^\top \text{sign}(\mathbf{b} - \mathbf{A}\mathbf{x}^{k-1}))_S\|_2^2 \\
&= \left(1 + \tau^2(\Phi^{-1} + \epsilon)^2(1 + \delta_s)^2 \mu_{k,0}^2 - 2c\sqrt{\frac{2}{\pi}} \left(\tau - \frac{|T_1^{k,0}|}{m} \right) (1 - \delta_s)\mu_{k,0} \right) \|\mathbf{x}_0 - \mathbf{x}^{k-1}\|_2^2 \\
&=: \beta_k \|\mathbf{x}^{k-1} - \mathbf{x}_0\|_2^2,
\end{aligned} \tag{B.7}$$

where $c = (2 - 2p)(1 - \delta_s) - (1 + \delta_s)$. Thus by substituting (B.5) and (B.7) into (B.4), we get the estimation (B.1).

(ii) Proof of the Inequality (B.2). It is clear that the estimation (B.2) comes from Proposition 3.1.

(iii) Proof of the Inequality (B.3). To prove (B.3), we first introduce an index set T^{s-k+1} , which corresponds to the $s - (k - 1)$ smallest values of $|(\mathbf{x}^{k-1} + t_{k,0}\mathbf{A}^\top \text{sign}(\mathbf{b} - \mathbf{A}\mathbf{x}^{k-1}))_j|$ for j in S . This allows us to derive a lower bound for ζ_k :

$$\begin{aligned}
\zeta_k &\geq \frac{1}{\sqrt{s - k + 1}} \|(\mathbf{x}^{k-1} + t_{k,0}\mathbf{A}^\top \text{sign}(\mathbf{b} - \mathbf{A}\mathbf{x}^{k-1}))_{T^{s-k+1}}\|_2 \\
&\geq \frac{1}{\sqrt{s - k + 1}} \left(\|(\mathbf{x}_0)_{T^{s-k+1}}\|_2 - \|(\mathbf{x}^{k-1} - \mathbf{x}_0 + t_{k,0}\mathbf{A}^\top \text{sign}(\mathbf{b} - \mathbf{A}\mathbf{x}^{k-1}))_{T^{s-k+1}}\|_2 \right).
\end{aligned}$$

Since $\|(\mathbf{x}^{k-1} - \mathbf{x}_0 + t_{k,0}\mathbf{A}^\top \text{sign}(\mathbf{b} - \mathbf{A}\mathbf{x}^{k-1}))_{T^{s-k+1}}\|_2 \leq \|(\mathbf{x}^{k-1} - \mathbf{x}_0 + t_{k,0}\mathbf{A}^\top \text{sign}(\mathbf{b} - \mathbf{A}\mathbf{x}^{k-1}))_S\|_2$ ($T^{s-k+1} \subseteq S$) and the estimation (B.7), we derive that

$$\zeta_k \geq \frac{1}{\sqrt{s - k + 1}} \left(\|(\mathbf{x}_0)_{T^{s-k+1}}\|_2 - \sqrt{\beta_k} \|\mathbf{x}^{k-1} - \mathbf{x}_0\|_2 \right).$$

Notice that (B.1) gives a lower bound of $\|(\mathbf{x}_0)_{(S^{k-1})^c}\|_2$, which depends on $\|\mathbf{x}^{k-1} - \mathbf{x}_0\|_2$. Given that $\beta'_k < 1/2$, we can establish the relationship of $\|\mathbf{x}^{k-1} - \mathbf{x}_0\|_2$ and $\|(\mathbf{x}_0)_{T^{s-k+1}}\|_2$ as follows

$$\begin{aligned}\|\mathbf{x}^{k-1} - \mathbf{x}_0\|_2 &\leq \frac{1}{\sqrt{1-2\beta'_k}} \|(\mathbf{x}_0)_{(S^{k-1})^c}\|_2 \leq \frac{\sqrt{s-k+1}}{\sqrt{1-2\beta'_k}} x_1^* \\ &\leq \frac{\sqrt{s-k+1}}{\sqrt{1-2\beta'_k}} \lambda x_s^* \leq \frac{\lambda}{\sqrt{1-2\beta'_k}} \|(\mathbf{x}_0)_{T^{s-k+1}}\|_2\end{aligned}$$

with the final inequality stemming from the fact that $\sqrt{s-k+1}x_s^* \leq \|(\mathbf{x}_0)_{T^{s-k+1}}\|_2$ and $T^{s-k+1} \subset S$. This implies that

$$\|(\mathbf{x}_0)_{T^{s-k+1}}\|_2 \geq \frac{\sqrt{1-2\beta'_k}}{\lambda} \|\mathbf{x}^{k-1} - \mathbf{x}_0\|_2. \quad (\text{B.8})$$

This allows us to deduce the estimation (B.3). Thus, we complete the proof. \square

B.2 Proof of Theorem 2.5

To end this section, we give the proof of Theorem 2.5.

Proof of Theorem 2.5. We define the set S as the support of \mathbf{x}_0 . Recall that ζ_k represents the k -th largest value of the elements in the subset S of $|\mathbf{x}^{k-1} + t_{k,0}\mathbf{A}^\top \text{sign}(\mathbf{b} - \mathbf{A}\mathbf{x}^{k-1})_j|$, while ξ_k denotes the largest value of the elements in the complementary subset S^c . Our objective is to establish that with high probability, $S^k \subseteq S$ for each $k \in [[s]]$. This is implied by the condition $\zeta_k > \xi_k$ for all $k \in [[s]]$. The probability of the event not holding is bounded by the following expression:

$$\begin{aligned}P &:= \mathbb{P}(\exists k \in [[s]] : \xi_k \geq \zeta_k \text{ and } (\zeta_{k-1} > \xi_{k-1}, \dots, \zeta_1 > \xi_1)) \\ &\leq \mathbb{P}\left(\left|\frac{\sqrt{\frac{\pi}{2}}\|\mathbf{A}\mathbf{x}\|_1}{\|\mathbf{x}\|_2} - 1\right| > \delta_s \text{ for some } s \text{ sparse } \mathbf{x}\right) \\ &\quad + \sum_{k=1}^s \mathbb{P}\left(\xi_k \geq \zeta_k, (\zeta_{k-1} > \xi_{k-1}, \dots, \zeta_1 > \xi_1), \left(\left|\frac{\sqrt{\frac{\pi}{2}}\|\mathbf{A}\mathbf{x}\|_1}{\|\mathbf{x}\|_2} - 1\right| \leq \delta_s \text{ for all } s \text{ sparse } \mathbf{x}\right)\right) \\ &=: P_1 + P_2,\end{aligned}$$

where the inequality comes from the probability formulation $\mathbb{P}(A) = \mathbb{P}(AB) + \mathbb{P}(A\bar{B}) \leq \mathbb{P}(AB) + \mathbb{P}(\bar{B})$. Referencing Lemma A.1, we find that P_1 is constrained by $2\exp(-\frac{\delta_s^2}{16}m)$.

Now we shift our attention to P_2 and employ the notation $\mathbb{P}(E)$ to denote the conditional probability of event E , given the intersection of two sets of conditions. The first set consists of the conditions $(\zeta_{k-1} > \xi_{k-1}, \dots, \zeta_1 > \xi_1)$, and the second set involves the event that the RIP₁ holds for all s -sparse vectors \mathbf{x} . We assume that these events are valid for the purpose of this analysis.

By Proposition 3.3, we get the estimation for P_2 as follows

$$P_2 \leq 2s(n-s) \exp\left(-\frac{\gamma_{k-1}^2 m}{6s}\right).$$

Combining these results, the overall failure probability P is bounded by

$$P \leq 2\exp\left(-\frac{\delta_s^2}{16}m\right) + 2s(n-s) \exp\left(-\frac{\gamma_{k-1}^2 m}{6s}\right).$$

In particular, we observe that $\zeta_k > \xi_k$, which implies $S^s = S$, with a failure probability not exceeding P . Furthermore, since $|\frac{\sqrt{\frac{\pi}{2}}\|\mathbf{A}\mathbf{x}\|_1}{\|\mathbf{x}\|_2} - 1| \leq \delta_s$ with a failure probability of $2\exp(-\frac{\delta_s^2}{16}m)$, we also find that

$$\begin{aligned}\|\mathbf{x}_0 - \mathbf{x}^s\|_2^2 &= \|(\mathbf{x}^s - \mathbf{x}_0)_{S^s}\|_2^2 + \|(\mathbf{x}^s - \mathbf{x}_0)_{(S^s)^c}\|_2^2 \\ &\leq 2\|(\mathbf{x}^s - \mathbf{x}_0 + t_{s+1,0}\mathbf{A}^\top \text{sign}(\mathbf{b} - \mathbf{A}\mathbf{x}^s))_{S^s}\|_2^2 \\ &\quad + 2t_{s+1,0}^2\|\mathbf{A}^\top \text{sign}(\mathbf{b} - \mathbf{A}\mathbf{x}^s)\|_2^2 + \|(\mathbf{x}_0)_{S^c}\|_2^2 \\ &\leq 2\beta'_{s+1}\|\mathbf{x}_0 - \mathbf{x}^s\|_2^2 + \|(\mathbf{x}_0)_{S^c}\|_2^2 \\ &< \|\mathbf{x}_0 - \mathbf{x}^s\|_2^2,\end{aligned}$$

where the second inequality is derived from (B.1) when $k = s + 1$, and the last inequality is from $(\mathbf{x}_0)_{S^c} = \mathbf{0}$ and $\beta'_{s+1} < 1/2$. Thus, we obtain $\mathbf{x}^s = \mathbf{x}_0$. The resulting failure probability is constrained by

$$\begin{aligned}4\exp\left(-\frac{\delta_s^2}{16}m\right) + 2s(n-s)\exp\left(-\frac{\gamma_{k-1}^2 m}{6s}\right) \\ \leq n\exp\left(-\frac{\delta_s^2}{16}m\right) + n^2\exp\left(-\frac{\gamma_{k-1}^2 m}{6s}\right) \\ \leq n^2\exp\left(-c'\frac{m}{s}\right) \\ \leq n^{-c''}.\end{aligned}$$

This bound holds with an appropriate selection of the constant c'_1 in the condition $m \geq c'_1 s \log n$. Thus we finish the conclusion. \square

References

- [1] Gilbert Bassett and Roger Koenker. Asymptotic theory of least absolute error regression. *J. Amer. Statist. Assoc.*, 73(363):618–622, 1978.
- [2] Peter J. Bickel, Ya’acov Ritov, and Alexandre B. Tsybakov. Simultaneous analysis of Lasso and Dantzig selector. *Ann. Statist.*, 37(4):1705–1732, 2009.
- [3] Peter Bloomfield and William Steiger. Least absolute deviations curve-fitting. *SIAM J. Sci. Statist. Comput.*, 1(2):290–301, 1980.
- [4] Thomas Blumensath and Mike E. Davies. Iterative thresholding for sparse approximations. *J. Fourier Anal. Appl.*, 14(5-6):629–654, 2008.
- [5] Thomas Blumensath and Mike E. Davies. Iterative hard thresholding for compressed sensing. *Appl. Comput. Harmon. Anal.*, 27(3):265–274, 2009.
- [6] Thomas Blumensath and Mike E. Davies. Normalized iterative hard thresholding: Guaranteed stability and performance. *IEEE J. Sel. Topics Signal Process.*, 4(2):298–309, 2010.
- [7] Jean-Luc Bouchot, Simon Foucart, and Paweł Hitczenko. Hard thresholding pursuit algorithms: Number of iterations. *Appl. Comput. Harmon. Anal.*, 41(2):412–435, 2016.
- [8] J. Bourgain and V.D. Milman. New volume ratio properties for convex symmetrical bodies in \mathbb{R}^n . *Inventiones Mathematicae*, 88(2):319–340, 1987.
- [9] T. Tony Cai and Anru Zhang. ROP: Matrix recovery via rank-one projections. *Ann. Statist.*, 43(1):102–138, 2015.

- [10] Rick Chartrand and Valentina Staneva. Restricted isometry properties and nonconvex compressive sensing. *Inverse Problems*, 24(3):035020, 2008.
- [11] Christian Clason and Bangti Jin. A semismooth newton method for nonlinear parameter identification problems with impulsive noise. *SIAM J. Imaging Sci.*, 5(2):505–536, 2012.
- [12] Fernando De La Torre and Michael J. Black. A framework for robust subspace learning. *Int. J. Comput. Vision*, 54(1):117–142, 2003.
- [13] Terry E. Dielman. Least absolute value regression: recent contributions. *J. Stat. Comput. Simul.*, 75(4):263–286, 2005.
- [14] Simon Foucart. Hard thresholding pursuit: an algorithm for compressive sensing. *SIAM J. Numer. Anal.*, 49(5/6):2543–2563, 2011.
- [15] Anna C. Gilbert, Howard W. Levinson, and John C. Schotland. Nonlinear iterative hard thresholding for inverse scattering. *SIAM J. Imaging Sci.*, 13(1):108–140, 2020.
- [16] W. Hoeffding. Probability inequalities for sums of bounded random variables. *Journal of the American Statistical Association*, 58:13–30, 1963.
- [17] Peter J. Huber and Elvezio M. Ronchetti. *Robust statistics*. John Wiley & Sons, 2011.
- [18] Xue Jiang, T. Kirubarajan, and Wen-Jun Zeng. Robust sparse channel estimation and equalization in impulsive noise using linear programming. *Signal Process.*, 93(5):1095–1105, 2013.
- [19] Liyuan Li, Weimin Huang, Irene Yu-Hua Gu, and Qi Tian. Statistical modeling of complex backgrounds for foreground object detection. *IEEE Trans. Image Process.*, 13(11):1459–1472, 2004.
- [20] Peng Li, Wengu Chen, Huanmin Ge, and Michael K. Ng. $\ell_1 - \alpha\ell_2$ minimization methods for signal and image reconstruction with impulsive noise removal. *Inverse Problems*, 36:055009, 2020.
- [21] Song Li, Dekai Liu, and Yi Shen. Adaptive iterative hard thresholding for least absolute deviation problems with sparsity constraints. *J. Fourier Anal. Appl.*, 29(5), 2023.
- [22] Yuanxin Li, Yuejie Chi, Huishuai Zhang, and Yingbin Liang. Non-convex low-rank matrix recovery with arbitrary outliers via median-truncated gradient descent. *Inf. Inference*, 9(2):289–325, 2020.
- [23] Yuanxin Li, Yue Sun, and Yuejie Chi. Low-rank positive semidefinite matrix recovery from corrupted rank-one measurements. *IEEE Trans. Signal Process.*, 65(2):397–408, 2016.
- [24] Ricardo A. Maronna, R. Douglas Martin, Victor J. Yohai, and Matías Salibián-Barrera. *Robust statistics: theory and methods (with R)*. John Wiley & Sons, 2019.
- [25] D. Needell and J. A. Tropp. CoSaMP: Iterative signal recovery from incomplete and inaccurate samples. *Appl. Comput. Harmon. Anal.*, 26(3):301–321, 2009.
- [26] Mila Nikolova. A variational approach to remove outliers and impulse noise. *J. Math. Imaging Vision*, 20(1-2):99–120, 2004.
- [27] Jose L. Paredes and Gonzalo R. Arce. Compressive sensing signal reconstruction by weighted median regression estimates. *IEEE Trans. Signal Process.*, 59(6):2585–2601, 2011.
- [28] Zhong-Feng Sun, Jin-Chuan Zhou, Yun-Bin Zhao, and Nan Meng. Heavy-ball-based hard thresholding algorithms for sparse signal recovery. *J. Comput. Appl. Math.*, 430:115264, 2023.

- [29] Andrew Wagner, John Wright, Arvind Ganesh, Zihan Zhou, Hossein Mobahi, and Yi Ma. Toward a practical face recognition system: Robust alignment and illumination by sparse representation. *IEEE Trans. Pattern Anal. Mach. Intell.*, 34(2):372–386, 2012.
- [30] Lie Wang. The L_1 penalized LAD estimator for high dimensional linear regression. *J. Multivariate Anal.*, 120:135–151, 2013.
- [31] Hang Xu, Song Li, and Junhong Lin. Convergence of projected subgradient method with sparse or low-rank constraints. *Adv. Comput. Math.*, 50(4), 2024.
- [32] Jiao Xu, Peng Li, and Bing Zheng. Matrix recovery from nonconvex regularized least absolute deviations. *Inverse Problems*, 40(6):065002, 2024.
- [33] Junfeng Yang and Yin Zhang. Alternating direction algorithms for ℓ_1 -problems in compressive sensing. *SIAM J. Sci. Comput.*, 33(1):250–278, 2011.
- [34] Xiao-Tong Yuan, Ping Li, and Tong Zhang. Gradient hard thresholding pursuit. *J. Mach. Learn. Res.*, 18(166):1–43, 2018.
- [35] Huishuai Zhang, Yuejie Chi, and Yingbin Liang. Provable non-convex phase retrieval with outliers: Median truncated wirtinger flow. In *Proceedings of The 33rd International Conference on Machine Learning (ICML)*, volume 48, pages 1022–1031, 2016.
- [36] Tong Zhang. Sparse recovery with orthogonal matching pursuit under RIP. *IEEE Trans. Inf. Theory*, 57(9):6215–6221, 2011.
- [37] Yanfeng Zhang, Yunbao Huang, Haiyan Li, Pu Li, and Xi'an Fan. Conjugate gradient hard thresholding pursuit algorithm for sparse signal recovery. *Algorithms*, 12(2):36, 2019.
- [38] Shenglong Zhou, Naihua Xiu, and Hou-Duo Qi. Global and quadratic convergence of newton hard-thresholding pursuit. *J. Mach. Learn. Res.*, 22(12):1–45, 2021.
- [39] Abdelhak M. Zoubir, Visa Koivunen, Esa Ollila, and Michael Muma. *Robust statistics for signal processing*. Cambridge University Press, 2018.